

1 **Long-term changes in a trochid gastropod population affected by biogenic sediment stability on an intertidal**
2 **sandflat in regional metapopulation context**

3

4 **Akio Tamaki¹, Seiji Takeuchi¹, Soonbo Yang², Shinji Sassa²**

5

6 **Affiliations:**

7 ¹ Graduate School of Fisheries and Environmental Sciences, Nagasaki University, Bunkyo-machi 1-14, Nagasaki 852-
8 8521, Japan

9 ² Port and Airport Research Institute, National Institute of Maritime, Port and Aviation Technology, 3-1-1 Nagase,
10 Yokosuka 239-0826, Japan

11

12 **Corresponding author:** Akio Tamaki; tamaki@nagasaki-u.ac.jp

13

14

15

16

17

18

19

20

21

22

23

24

25

26 **Abstract**

27 Although destabilization and stabilization of soft sediments by macro-infauna are regarded as key to understanding
28 benthic community dynamics, how component populations are affected concurrently by both agents was poorly
29 investigated. On an intertidal sandflat, Kyushu, Japan during 1979–2014 (previous study) and 2015–2019, monitoring
30 was made of the populations of the filter-feeding gastropod, *Umbonium moniliferum*, the burrow-dwelling ghost shrimp,
31 *Neotrypaea harmandi* (destabilizer), and the tube-building polychaete, *Mesochaetopterus minutus* (stabilizer). Results
32 revealed that gastropod population changes were driven by an interplay of shrimp, polychaete, and the stingray,
33 *Hemirhynchus akajei*, foraging for shrimp by sediment excavation. The gastropod went through high abundance (1100
34 m⁻²) in 1979, extinction during 1986–1997, two marked recoveries with peaks in 2001 and 2009, a slight recovery in
35 2016, and near extinction in 2019. These changes largely followed the fluctuation in shrimp density across a threshold
36 of 160 m⁻² inhibiting gastropod recruitment. The polychaete exhibited intermittent outbreaks with peaks in 2000, 2007,
37 and 2016, with maximum densities of 15000–24000 m⁻². Sandflat topography and sedimentary variables were measured
38 during 2015–2017. Sediment stabilization by polychaete aggregations at the mid-tidal zone is suggested to have boosted
39 gastropod recruitment. Release at sea and retrieval on shore of drift cards mimicking gastropod larvae with 3–9-d
40 planktonic duration was conducted in 2008–2009 to specify source populations sending larvae to the present population.
41 Potential source populations were censused in 1998 and 2017–2018. Their recent virtual extinction appears responsible
42 for the present population’s decline from 2011. This raises the need for metapopulation perspective to understand local
43 dynamics.

44

45 **Introduction**

46 Destabilization and stabilization of soft sediments by physical and biological agents are one combination of key
47 processes affecting population and community dynamics of many benthic invertebrates and their surrounding ecosystem
48 (Rhoads 1974; Woodin and Jackson 1979; Reise 2002; Bouma et al. 2009; Berke 2010). Of the biological agents,
49 sediment destabilizers are often regarded as synonymous with bioturbators (Jones et al. 1994; Berke 2010), though
50 broader types of benthic functional groups are included in the latter. Dense aggregations of tube builders are usually

51 regarded as sediment stabilizers, whereas at low densities, they can cause erosion of sediment (Eckman et al. 1981). Of
52 the tube builders, hereafter excluded from consideration are two taxonomic groups of constructors of firm reef patches:
53 sabellariid polychaetes (e.g., *Sabellaria* spp.) and serpulid polychaetes (e.g., *Ficopomatus* spp.). Only assemblages of
54 less rigid tubes merging into the ambient sediment are targeted. It is poorly understood how any population in a benthic
55 community is affected concurrently by those sediment destabilizers and tube builders at high densities.

56 On intertidal sandflats, callianassid shrimp (or ghost shrimp) are one typical sediment destabilizer that has a large
57 body size and resides in relatively deep burrows (Feldman et al. 2000; Flach and Tamaki 2001; Pillay and Branch 2011).
58 Species of this family affect members of other functional groups of macrofauna in different ways, killing or expelling
59 small tube builders (Tamaki 1985; Posey 1986; Wynberg and Branch 1994; Berkenbusch et al. 2000; Pillay et al. 2007a)
60 and filter-feeding molluscs (Murphy 1985; Tamaki 1994; Dittmann 1996; Berkenbusch et al. 2000; Dumbauld et al.
61 2006; Pillay et al. 2007a,b; Takeuchi et al. 2013; Hanekom and Russell 2015), while accommodating small mobile
62 forms by making sediments less packed or more oxygenated and oxidized (Tudhope and Scoffin 1984; Posey 1986;
63 Riddle 1988; Tamaki and Suzukawa 1991; Wynberg and Branch 1994; Tamaki et al. 2018b).

64 One adaptive significance of tube-building habit in soft-sediment benthos would be to resist water turbulence,
65 sediment shifting, and predation. Regarding populations of tube-building species, spatial and temporal variations in
66 their sizes, abundances of associated species populations, and community structure around them have been highlighted
67 for polychaetes (Fager 1964; Bailey-Brock 1979; Wilson 1979; Woodin 1981; Gallagher et al. 1983; Cummings et al.
68 1996; Bolam and Fernandes 2003; Alves et al. 2017), amphipods (Mills 1967; Reise 1978; Wilson 1989; Mackenzie et
69 al. 2006; Rigolet et al. 2014), tanaid (Gallagher et al. 1983), and phoronid (Everett 1991). These tube builders provide
70 smaller macrobenthos of varying mobilities with more immobilized sedimentary or food-richer (e.g., benthic
71 microalgae) microhabitats under disturbed substrates, except for inhibitory effects of spionids or corophiids on larval
72 settlement (e.g., by predation) or of inducing emigration of juveniles or adults of other species. One facilitative aspect of
73 these tube builders' aggregations on other benthos is exhibited in enhanced planktonic larval deposition by water flow
74 attenuation or in provision of accommodation for mobile juveniles (Gallagher et al. 1983; Armonies and Hellwig-
75 Armonies 1992; Bolam and Fernandes 2003; Volkenborn and Reise 2007).

76 On intertidal sandflats where ghost shrimp and tube builders meet, amensalism from the former to the latter is
77 prevalent (second par.). Although a laboratory experiment demonstrated retardation of burrowing of ghost shrimp into
78 sediment with dense tube mats (Brenchley 1982), no field data have been published about any reciprocal effect of tube
79 builders on adults of ghost shrimp (Flach and Tamaki 2001; Pillay and Branch 2011). Most tube builders are smaller
80 than ghost shrimp in size, and only at high densities could they affect ghost shrimp negatively in the field (e.g., by a
81 chaetopterid polychaete, but with photograph only: Tamaki and Takeuchi 2016). Therefore, spatial and temporal
82 changes in population size of any one tube-building species would be subjected to population dynamics of ghost shrimp.
83 What scarce circumstances may allow tube builders to establish in a ghost shrimp bed? Changes in a tube builder
84 population in response to that in a ghost shrimp population may have knock-on effects on populations of other members
85 of the benthic community, including those on populations of species associated with a tube builder's aggregations, but
86 no such effects are known. In addition, in the recruitment of planktonic larvae of any species affected by dominant
87 biogenic sediment modifiers, local populations that supply those larvae of auto- and/or allo-chthonous origins have
88 rarely been specified in a regional metapopulation (cf., Heino et al. 2015; Tamaki and Takeuchi 2016).

89 In Kyushu, Japan, the benthic community of an intertidal sandflat (called Tomioka sandflat) was monitored every
90 spring and summer during 1979 to 2014 (Tamaki and Takeuchi 2016). The most dominant species was the callianassid
91 shrimp, *Nihonotrypaea harmandi*, of which generic assignment was recently moved to *Neotrypaea* (Poore et al. 2019).
92 Along with a marked increase in ghost shrimp density and distribution range from 1979 onward, the epibenthic filter-
93 feeding trochid gastropod, *Umbonium moniliferum*, another dominant community member, with many associated
94 species, went extinct in 1986 (Tamaki 1994). Afterward, the density of ghost shrimp, but not the distribution range,
95 began to decrease from 1995, reaching the 1979-level in 1998 (Tamaki and Takeuchi 2016; Tamaki et al. 2020a). This is
96 attributable to markedly increased predation by the stingray, *Hemitrygon akajei*, from 1994 (Takeuchi and Tamaki 2014;
97 Tamaki et al. 2020a). Stingrays excavate large pits to catch infaunal prey, which causes sediment destabilization to
98 much greater magnitudes than infaunal destabilizers do, adding complexity to sediment re-distribution over tidal flats
99 (see references listed in Takeuchi and Tamaki 2014). The effect of sediment destabilization caused by vertebrate
100 predators on macrobenthic populations and communities has been studied sporadically (reviewed by Tamaki and

101 Takeuchi 2016). The *U. moniliferum* population on Tomioka sandflat began to recover from 1997, attaining discrete
102 peak densities in 2001 and 2009, of which values were comparable to that in 1979 (Mandal et al. 2010; Tamaki and
103 Takeuchi 2016). Local gastropod populations supplying larvae to the Tomioka sandflat population in these recovery
104 phases were considered to lie within 20 km from the sandflat (Tamaki and Takeuchi 2016), of which larval transport
105 process remains to be examined. On Tomioka sandflat, marked decreases in gastropod density occurred between 2001
106 and 2009, and after 2009. That first decrease corresponded with the temporary increase in ghost shrimp density, but the
107 second decrease took place under the lower shrimp densities. The rise and fall in population size of the gastropod nearly
108 coincided with that of a suspension-feeding chaetopteric polychaete, *Mesochaetopterus minutus*, which formed tube
109 aggregations around the mid-intertidal, *U. moniliferum* larval settlement zone (Tamaki and Takeuchi 2016). This worm
110 has a wide geographic distribution and is present in the Pacific and Indian Oceans (Biseswar et al. 2002; Bhaud 2005).
111 Locally it and *M. sagittarius* provide other benthos with immobilized sediment patches, increasing species richness and
112 individual abundance [Biseswar et al. (2002) and Bailey-Brock (1979), respectively]. Tamaki and Takeuchi (2016)
113 inferred the existence of inhibition of worm recruitment by ghost shrimp and of facilitation of gastropod recruitment in
114 worm aggregations in the midst of the ghost shrimp bed on Tomioka sandflat. After 2014, monitoring of the benthic
115 community continued until 2019, during which time the third worm outbreak occurred (A. Tamaki, unpubl data). This
116 provides an opportunity to examine whether another recovery of the gastropod population occurred in its regional
117 metapopulation and to find a clue to how sediment stabilization by the worm could, if any, boost gastropod recruitment.

118 The aim of the present study was to check a 40-y consistency of inhibition of both *U. moniliferum* and *M. minutus*
119 recruitment by dense *N. harmandi* assemblages and of facilitation of *U. moniliferum* recruitment by worm aggregations
120 in the ghost shrimp bed on Tomioka sandflat. Results of the census of these species populations during 2015 to 2019
121 were compared with the previous ones during 1979 to 2014. Sediment grain-size composition, hardness, and surface
122 topographies were measured to examine the effects of sediment stabilization by the worm and destabilization by the
123 ghost shrimp and the stingray (*H. akajei*) on gastropod recruitment. The possibility of gastropod larval transport from
124 several intertidal sandflats to Tomioka sandflat was tested by drift card release and retrieval. Those former sandflats'
125 populations were censused to assess their potential to serve as a demographic source in the regional metapopulation.

126

127 **Materials and methods**

128 **Study region and areas**

129 The study region was part of an estuary–coastal ocean system in mid-western Kyushu, ranging from the outer one-
130 third part of Ariake Sound to Amakusa-nada off Amakusa-Shimoshima (A.-S.) Island (Fig. 1a). This region is under a
131 meso-tidal and mixed, mainly semidiurnal, tidal regime (Fujimoto 1990). The average tidal range in Amakusa-nada in
132 spring tide periods is 3 m. Tomioka (intertidal) sandflat is located at the head of Tomioka Bay on the northwestern
133 corner of A.-S. Island. The bay spans 8.5 km alongshore and 2 km across the shore. M_2 (largest lunar constituent) is
134 most dominant in the tidal current between Amakusa-nada and Ariake Sound, with much prevalence of east–west over
135 north–south components close off Tomioka Bay (Fujiie et al. 2006). The highest surface water velocities are 150 cm s^{-1}
136 at the narrow inlet to Ariake Sound (Hayasaki Straits) located 10 km east of the bay, and 60 and 20 cm s^{-1} in the bay in
137 spring and neap tide periods, respectively (Tamaki et al. 2018a, 2020b). The sandflat is emersed maximally 150–550 m
138 offshore and 3.5 km alongshore (Fig. 1b). The main population census area for the three target species was the sandflat
139 northwestern corner, spanning 500 m along the shoreline (Fig. 1c). Intertidal sandflats with *U. moniliferum* populations
140 which would have sent larvae to the Tomioka population in its recoveries in the 2000s lie on the eastern shoreline of A.-
141 S. Island in Ariake Sound, which are 10–20 km (south)east of Tomioka Bay (Fig. 1d; Tamaki and Takeuchi 2016).

142

143 **Information on three benthic species populations in regional waters and intertidal sandflats**

144 Each adult of *N. harmandi* (to 45-mm total length) dwells singly in a Y-shaped burrow in the whole sand column
145 reaching 30–60 cm below the surface (Tamaki and Ueno 1998; two surface burrow openings correspond to one shrimp;
146 below the sand column lies shell hash). The reproductive season is from June through October, and newly-hatched
147 larvae are transported to the nearby coastal ocean (Amakusa-nada; Fig. 1a) (Tamaki et al. 1997, 2020b). Two major
148 newly-recruited cohorts occur per season, in July to August (first 0-y cohort) and September to October (second 0-y
149 cohort). It takes nearly 1 y for each cohort to become mature (first and second 1-y cohorts). These cohorts merge into a
150 single cohort by early June of the second year (2-y cohort), reproduce, and die off by the end of summer; hereafter any

151 shrimp with one calendar-year shift is called a 1- or 2-y cohort member. The Tomioka population was estimated to
152 account for 70% of the regional metapopulation in size in 1998 (Tamaki and Harada 2005). The threshold *N. harmandi*
153 density inhibiting *U. moniliferum* recruitment was estimated to be 160 shrimp m⁻², based on the census of local
154 populations other than the Tomioka population (Tamaki and Takeuchi 2016). This shrimp density consistently applied to
155 the shrimp and gastropod populations on Tomioka sandflat, with changes in *U. moniliferum* population size during 1979
156 to 2014 following those in shrimp densities across that threshold value (Tamaki and Takeuchi 2016). Adults of *U.*
157 *moniliferum* (to 14-mm shell width) mainly inhabit the population census area of Tomioka sandflat (Fig. 1c), occupying
158 its lower-half zone of a 300-m range between tide marks (Tamaki and Kikuchi 1983). Mass spawning of gametes occurs
159 discretely, centered at each of the three serial neap tide periods from the end of September to early November (Mandal
160 et al. 2010). It takes a minimum of 3 d for lecithotrophic planktonic larvae to settle on the sandflat. The settlement
161 continues substantially up to 9 d after gamete fertilization. Both neap-tide gamete spawning under the weakest tidal
162 currents of the semilunar cycle and short planktonic larval duration suggest some larval retention in a natal embayment.
163 In Tomioka Bay, the density-weighted average larval depth in the water column was between 7 and 12.5 m, with 25% of
164 the larvae present in the surface 1-m layer. The three juvenile cohorts on the sandflat merge into a single cohort (0+ old
165 cohort) by April, reaching maturity in October. Ten intertidal populations in Ariake Sound were regarded as candidates
166 sending larvae to Tomioka population during its recovery phases in the 2000s (Tamaki and Takeuchi 2016). Of these,
167 six populations on the eastern shoreline of A.-S. Island were most likely candidates (U2 to U7 sandflats in Fig. 1d).
168 Individual tube diameter of *M. minutus* is up to 1.0 mm. Tube-aggregation forms vary from a cluster with bumpy
169 sandflat surfaces (Fig. 2) to a dome-shaped mound with accumulated sediment (Tamaki and Takeuchi 2016, fig. 14B).

170 Further information on *U. moniliferum* and *M. minutus* is compiled in Supplementary material 1 and 2, respectively.

171

172 **Census of three benthic species populations on Tomioka sandflat**

173 Individual densities of *N. harmandi*, *U. moniliferum*, and *M. minutus* were monitored along Transect G on Tomioka
174 sandflat (Fig. 1c) during emersed times in spring tide periods each year from 2015 to 2019: March 21 and August 1 in
175 2015, May 22 and August 2 in 2016, March 1 and 30, and July 23 in 2017, July 13 and August 10 in 2018, and August 2

176 in 2019. The representativeness of that transect for the whole census area with respect to the distributions of these
177 species was based on their zonal patterns quasi-parallel to the shoreline (e.g., Tamaki and Kikuchi 1983; Tamaki 1994;
178 Tamaki et al. 2018b). A total of 16 (as a rule) sampling stations was placed on the transect (hereafter the station X m
179 seaward of the upper shoreline is termed Stn X). Except for the segment from Stn 0 to Stn 10, two adjacent stations were
180 20 m apart between Stn 10 and Stn 290 located at MLWS (mean low water level in spring tide periods). For estimating
181 *N. harmandi* densities, burrow openings on the sandflat surface were counted for six to nine contiguous 25- × 25-cm
182 square plots at a randomly chosen spot around each station. The surface with apparent signs of recently made stingray
183 pits were avoided. For the other two species, one plot per station was enclosed with a metal quadrat frame of the same
184 size as above to 10-cm depth, and the inside cohesive sediment blocks were taken with a plasterer hoe with a 18- × 16-
185 cm blade and washed through a 0.5-mm mesh sieve. The residue was fixed with 10% neutralized formalin solution. On
186 March 1, 2017, the sandflat was emersed to Stn 230, and only counting shrimp burrow openings was made. The count
187 for Stns 250, 270, 280, and 290 and the collection of the gastropod and worm at the 16 routine stations were made on
188 March 30. In 2018, the shrimp burrow-opening count was made on July 13, but not on August 10, when macrobenthos
189 was collected. On August 3, 2016 and May 27, 2017, to examine actual shrimp densities and cohort compositions at
190 each of Stns 30, 90, 150, 210, and 270, ten sediment columns to their bottom layers were taken with an acrylic tube with
191 a 100-cm² cross-sectional area and 80-cm length, individually sieved, and fixed in the same manner as above. To
192 confirm that aggregations of *M. minutus* were distributed in the mid-tidal zone parallel to the shoreline and whether
193 areal variation in worm densities were related to that in *N. harmandi* densities, in addition to the 16 points along
194 Transect G (on August 2), 46 points in and around that zone were surveyed during low tide on August 1, 2016. The
195 geographical positions of these points were determined with eTrex 10J (Garmin). At each point, (1) one sediment
196 sample for the worm was collected with an acrylic tube with a 100-cm² cross-sectional area to 10-cm depth, washed
197 through a 0.5-mm mesh sieve, and fixed with formalin, (2) ghost shrimp burrow openings were counted for four 25- ×
198 25-cm square plots, and (3) some sediment clod for granulometric analysis was taken to 1-cm depth at each of six
199 randomly chosen points. To examine the vertical dimension of *M. minutus* tubes, at Stn 160 on May 13, 2017, (1)
200 heights above the ground were measured with a ruler to 1 mm ($n = 20$) and (2) each of three sediment cores with a 100-

201 cm² cross-sectional area to 25-cm depth was cut into the 25–20, 20–15, 15–10, and 10–0-cm layers, washed through 1-
202 mm mesh sieves, and fixed for later analysis of tube mass weight by each depth layer.

203

204 **Sediment properties and surface topography on Tomioka sandflat**

205 Along with the above quadrat sampling on Transect G, during 2015 to 2018, some sediment clod was collected for
206 granulometric analysis to 1-cm depth and also to 3 cm on several occasions (only 3 cm in August 2015). At each station,
207 during ± 1 h around the lowest-tide time on August 1, 2015, August 2, 2016, and March 30, 2017 (weather was fine and
208 calm), after a flat surface was shoveled, with the stop of seepage of groundwater, its table level was measured to 1 mm
209 with a ruler. Following Sassa et al. (2011), sediment hardness at 1-cm and 4-cm depths was measured with a vane blade
210 of 40-mm ϕ , 10-mm depth, and 0.5-mm thickness (FTD2CN-S, Seiken) and of 20-mm ϕ , 40-mm depth, and 0.5-mm
211 thickness (FTD5CN-S, Seiken), respectively, at a point randomly placed between surface burrow openings of *N.*
212 *harmandi*. In addition, in a few-m² area near Stn 170 of Transect G in 2016, sediment hardness to 1-cm depth was
213 measured at several points in and out of *M. minutus* aggregations, with varying groundwater tables for each group.

214 Ground heights over Tomioka sandflat relative to mean sea level in Tokyo Bay were measured with TRIMBLE R4
215 GNSS System (Trimble; precisions to 3 mm horizontally and 5 mm vertically) over part of the benthic population
216 census area including Transect G every 23 to 90 m on August 1, 2015 (310-m shore-normal \times 270-m alongshore
217 rectangular area) and 25 m on August 2, 2016 (300 m \times 350 m). Heights at the stations on Transect G were measured
218 more closely (every 10 m, 10 to 20 m, and 20 m in 2015, 2016, and on July 23, 2017, respectively). In addition, (1) in
219 an area around Stns 150 and 170 of Transect G in 2016 and 2017, measurement with a finer resolution (every 2 to 3 m)
220 was made for each of two adjacent strips (maximally 13-m shore-normal \times 54-m quasi-parallel to the shoreline and 16
221 m \times 69 m, respectively) and (2) in 2016, for one elevated plot with numerous worm tubes near Stn 170, detailed
222 measurement was made at 44 points with TOPCON GSX2 GNSS System (Topcon; precisions to 10 mm horizontally
223 and 15 mm vertically). Furthermore in 2016, aerial photographs of part of the sandflat were taken from 10s-m heights
224 near Stn 170 of Transect G with the use of a drone [PHANTOM3 Standard (DJI), 72-dpi image resolution].

225

226 **Census of *N. harmandi* and *U. moniliferum* populations on intertidal sandflats other than Tomioka sandflat**

227 Five of the U_n (n = identity number, 1 to 7) sandflats on the eastern shoreline of A.-S. Island were surveyed for *N.*
228 *harmandi* and *U. moniliferum* populations during low tides in 2017–2018 (Fig. 1d): in 2017, U2 and U3 (July 25), U5
229 (July 23), and U6 (July 22); in 2018, U7 (May 15–16). On U2, U3, U5, and U6 sandflats, sampling was conducted on
230 one or two shore-normal transects along the tidal gradient, covering the segment from mid-zone to upper part of the
231 lower zone potentially inhabitable by adult gastropods (red lines in Fig. 1d). Adjacent sampling stations were placed
232 quasi-distant apart. On U7 sandflat, with its tidal gradient in multiple directions, sampling stations were placed wide
233 over a substantial area (red plots in Fig. 1d). At each of a total of 30 stations on U6 sandflat, surface burrow openings of
234 ghost shrimp in four contiguous plots with a 25- × 25-cm unit square area were counted, and the sediment of one plot
235 enclosed with a quadrat frame was excavated to 5-cm depth, washed through a 1-mm mesh sieve, and fixed with 10%
236 neutralized formalin solution. At each station on U2 (8 stns), U3 (7 stns), and U5 (10 stns) sandflats, burrow openings
237 were not counted, and ten 10- × 10-cm square areas were excavated to 2-cm depth and sieved together. At each of the 24
238 stations on U7 sandflat, shrimp burrow openings were counted for nine quadrat plots, and benthos were collected with a
239 tube with a 100-cm² cross-sectional area to 10-cm depth (n = 6) and washed together through a 0.5-mm mesh sieve. The
240 above inconsistency in sampled sediment depths and sieve meshes does not affect the comparison among the gastropod
241 populations because of its epibenthic habit and adult shell widths of >1 mm (Tamaki and Takeuchi 2016).

242

243 **Drift card release in waters off several intertidal sandflats and retrieval on Tomioka sandflat**

244 To examine the possibility that substantial numbers of *U. moniliferum* larvae are retained in Tomioka Bay and
245 transported to the bay from several intertidal sandflats on the eastern shoreline of A.-S. Island (Fig. 1) within gastropod
246 planktonic larval duration (PLD) estimated from larval developmental durations in the laboratory (Mandal et al. 2010),
247 drift cards were released from around the above locations during October–November in 2008 and 2009. Later, those
248 stranded on Tomioka sandflat were retrieved. The card was intended to mimic a larva in the surface 1 m of the water
249 column. It is a 0.25-mm thick, yellow-colored biodegradable paper with a water-repellent coating, 10.0 cm × 14.8 cm in
250 size and 3.5 g in weight (Heiwado Printing, Tokyo), with a 0.9-g weight attached to one corner. In seawater, the card

251 stood upright, with the corner opposite to the weighted one 1 cm above the surface. The areal ratio of above to below
252 surface parts less than 0.01 would guarantee that card drift is not neustonic (Fukushima 2006). On each occasion, cards
253 were dropped off a 5-t fisherman's boat in order, from Tomioka Bay points to several points close off U1 to U7 of the
254 eastern shoreline of A.-S. Island, at around each local high-tide time (release points will be mapped in the Results). The
255 high-tide time for U7 is ca. 50 min behind that for Tomioka Bay. The high-tide time of the daily tidal cycle was adopted
256 for the release, based on both laboratory and field observations on the gastropod synchronized spawning time (Mandal
257 et al. 2010). At these times of card release, the weather was fine and sensible winds were weak, suggesting that the
258 initial card transport ashore by northeasterly wind-driven water currents was less than offshore transport by ebb tidal
259 currents. In 2008, card release was made during 0943 to 1112 hr on October 3 (in mid-tide period 4 d after the syzygy),
260 with 6000 cards at one Tomioka Bay point and 1000 cards at each of the other four points [off U1 and U2 ('and':
261 sandflats as a combined group), U3, U4 and U5, and U6 and U7]. In 2009, release was made twice: (1) during 0507 to
262 0627 hr on October 15 (in mid-tide period 4 d after the quadrature), with 1000 cards at each of one Tomioka Bay point
263 and five other points (off U1 and U2, U3, U4, U5, and U6 and U7); (2) during 1551 to 1705 hr on October 27 (in neap
264 tide period 1 d after the quadrature), with 800 cards at each of two Tomioka Bay points (the previous point and another
265 one closer to the sandflat: 550 m and 260 m off, respectively) and three other points (off U1, U2 and U3, U4 and U5,
266 and U6 and U7). For each card release, retrieval started the next day and continued daily: in 2008, from October 4 to 22;
267 in 2009, from October 16 to 20 (for the first release) and from October 27 to November 3, November 4 and 5, and
268 November 12 and 13 (for the first and second). Almost all retrieved cards had been stranded around the high-tide lines
269 on each previous date, not on its seaward, emerged part of the sandflat. Retrieval was conducted along the upper
270 shoreline of a main part of Tomioka sandflat (the actual part will be mapped in the Results), of Tomoé Cove, and of the
271 outer sand spit facing Tomioka Bay (from spit base across the innermost cove to tip) (Fig. 1b) from 3 h before the
272 daylight lowest-tide time to around that time by two persons (except for three on one occasion) of five regular members.

273

274 **Laboratory analysis for benthos distribution and abundance, sediment properties, and sandflat topography**

275 Specimens of *M. minutus* and *U. moniliferum* were enumerated. For the worm tubes contained in each of the four

276 sediment depth layers, blotted wet weights were measured to 0.1 g. Gastropod shell widths were measured with Vernier
277 caliper to 0.1 mm for individuals ca. ≥ 3 mm and with eyepiece micrometer in stereomicroscope to 0.05 mm for those < 3
278 mm (round to 0.1 mm) and their frequency distribution combined from all stations of Transect G on Tomioka sandflat
279 made for each sampling occasion, with a class interval of 0.4 mm. For most occasions, 0+ old cohort and 1+ and older
280 cohort were well separated (see Supplementary material 1 for cohort designation). In cases for some overlap in size
281 between the two cohorts (e.g., Tamaki and Takeuchi 2016, fig. 10), the gastropod number of 0+ old cohort in its possible
282 maximum shell-width class was estimated by linear interpolation between the total number in its left adjacent class and
283 zero in its right adjacent class. For the samples of *N. harmandi* individuals collected directly by coring on Tomioka
284 sandflat, the shrimp total length-frequency distributions were made according to Tamaki et al. (1997).

285 Based on the above data set together with the surface burrow-opening count data for ghost shrimp, the distribution
286 and abundance pattern of the three target benthic species on Tomioka sandflat and five *Un* sandflats of the eastern
287 shoreline of A.-S. Island were examined. In depicting the distributions of densities of *N. harmandi*, *M. minutus*, and *U.*
288 *moniliferum* over Transect G on Tomioka sandflat during 2015 to 2019, data in August 2010 were added to each
289 species' distribution profile as a reference, adapted from Tamaki et al. (2018b, fig. 5), Tamaki and Takeuchi (2016, fig.
290 13), and Tamaki and Takeuchi (2016, fig. 10), respectively. For *N. harmandi*, (1) shrimp densities were estimated from
291 surface burrow openings and (2) unit area for mean density at each station was converted from 625 cm² to 1 m², in
292 which a low (SD/mean) value for burrow-opening counts had guaranteed the representativeness of the mean value for
293 the 1979 to 2014 [mean of 0.22 for those (SD/mean)s: Tamaki and Takeuchi (2016, fig. 7)]; the values after 2014 will be
294 given in the Results. For *M. minutus* and *U. moniliferum*, the numbers of worms and gastropods of 0+ old cohort and 1+
295 and older cohort per 625 cm² at each station were used. To depict the yearly change in the abundance of each of the
296 three species representative of Transect G during 1979 to 2019, a measure over all stations (mostly 16) on every
297 sampling occasion was defined, as follows (the values for the 1979 to 2014 were adapted from Tamaki and Takeuchi
298 2016, fig. 11A–D). For the abundance measure of *N. harmandi*, mean (\pm SD) density over all stations was adopted, in
299 which the value for each year from 1979 to 2014 was an estimate for the non-existent value for October (month of the
300 year for gastropod reproduction, hereafter termed 'putative October'), being set the same as the real value in the

301 following March (Tamaki and Takeuchi 2016). The rationale for this treatment is the much higher survival rate of
302 shrimp during November to March than in the other months of the year (Tamaki et al. 1997). For the years with no
303 March data, the summer value of each same year was used. For each sampling occasion from 2015 to 2019, the real
304 value was adopted (the value for March 21, 2015 is identical to that for putative October 2014). For the abundance
305 measure of *M. minutus*, the total number of worms over all stations with a 1-m² sum area (= 625 cm² × 16) was adopted,
306 in which the value in July or August and that on every sampling occasion were used for the 1979 to 2014 and the 2015
307 to 2019, respectively. For the abundance measure of *U. moniliferum*, the total number of individuals of 0+ old cohort
308 and that of all cohorts over the transect stations were adopted, in which the values in July or August and those on every
309 sampling occasion were used for the 1979 to 2014 and the 2015 to 2019, respectively. Hereafter for *M. minutus* and *U.*
310 *moniliferum*, the term, ‘the abundance’ is used to designate each specific measure versus the use of ‘abundance’ as a
311 general term.

312 The effects of adults of *N. harmandi* (ghost shrimp) and adults of *M. minutus* (worm) on the recruitment of *U.*
313 *moniliferum* (gastropod) over Transect G on Tomioka sandflat would vary, depending on spatial variations in the density
314 of these adults and in the density of newly-settled gastropod juveniles primarily sorted by hydrodynamics. Following
315 Tamaki and Takeuchi (2016), a coefficient of permission for gastropod recruitment by the shrimp over the transect [CP
316 (shrimp→gastropod); 0 ≤ CP ≤ 1] was defined as $\Sigma [(term-1) \times (term-2)]$ for all (16) stations on Transect G, where term-1
317 is the relative degree of gastropod recruitment success corresponding to the four classes of ghost shrimp density (GSD:
318 shrimp m⁻²) at each station, which is 1, 0.23, 0.18, and 0 for 0 ≤ GSD < 50, 50 ≤ GSD < 100, 100 ≤ GSD < 160, and 160 <
319 GSD, respectively, and term-2 is a fixed numerical proportion of newly-settled gastropods at each station according to
320 their allocation over the transect by hydrodynamic sorting (Tamaki and Takeuchi 2016, fig. 9B; Σ proportions = 1).
321 Regarding term-2, CP values are most affected by the higher proportions of juvenile gastropod occurrence at the four
322 mid-transect stations (i.e., Stns 130 to 190). A coefficient of possible boost for gastropod recruitment by the worm [CPB
323 (worm→gastropod)] was defined as $\Sigma [(term-1') \times (term-2')]$ for all transect stations, where term-1' is worm density
324 (worms m⁻²) at each station, and term-2' is the same as term-2 in CP.

325 For the mid-tidal zonal area containing *M. minutus* aggregations on Tomioka sandflat, inverse-distance-weighted

326 interpolation of worm and ghost shrimp densities were made with 'idw' function in 'gstat' package of 'R' ver. 3.2.3 (R
327 Core Team 2015), in which the uppermost five and lowermost two stations on Transect G were excluded from analysis.

328 Granulometric analysis for sediment samples from Tomioka sandflat was made using a laser diffraction particle-size
329 analyzer (SALD-3100, Shimazu) to determine three parameter values [median phi ($Md\phi$), sorting coefficient (σ_1 :
330 inclusive graphic standard deviation; Buchanan and Kain 1971), and silt-clay or mud content in volume (<0.063 mm in
331 diameter)]. In depicting the distributions of these parameters over Transect G during 2015 to 2019, data in August 2010
332 were added to each distribution profile as a reference, adapted from Tamaki et al. (2018b, fig. 6). Analysis was made
333 also for a mass of sediment grains scraped off several tube sheaths of *M. minutus* secretion collected at each of the six
334 points with sediment samples for grain size compositions in the areal worm and ghost shrimp survey in August 2016.

335 For Tomioka sandflat, the isobaths of ground heights over a 280- × 280-m area around Transect G in August 2015
336 and August 2016 and those over the two mid-shore strips and the single elevated topography measured with the finer
337 resolution in 2016 and 2017 were made with the kriging interpolation option in Surfer 12 (Golden Software).

338

339 **Results**

340 **The abundances of ghost shrimp and worm on Tomioka sandflat**

341 Based on each population abundance measure representative of Transect G on Tomioka sandflat on every sampling
342 occasion from 1979 to 2019, yearly changes in (a) mean (\pm SD) density of *N. harmandi* (ghost shrimp), (b) the
343 abundance of *M. minutus* (worm), (c) CP (shrimp→gastropod) and CPB (worm→gastropod), and (d) the abundance of
344 *U. moniliferum* (gastropod) are shown in Fig. 3a–d, respectively. The mean (\pm SD) values for the (SD/mean) values of
345 shrimp surface burrow-opening densities over all transect stations on the seven occasions from August 2015 to August
346 2019 were 0.34 (0.16), 0.28 (0.08), 0.26 (0.09), 0.21 (0.07), 0.26 (0.10), 0.24 (0.09), and 0.20 (0.10), respectively, of
347 which mean values were near to those for the 1979 to 2014 (the Materials and methods, last sub-sect.).

348 Ghost shrimp mean density increased markedly from 1979 to 1984, crossing the empirical threshold density (160
349 shrimp m^{-2} above which gastropod recruitment is inhibited) between 1980 and 1981 and peaking at 626 shrimp m^{-2} in
350 1988. From 1988 to 2001, the population was largely on the decline, crossing the threshold between 1997 and 1998.

351 From 2001 to 2014, the rising and falling phases came alternately, with the period above the threshold between 2002
352 and 2007 and in 2014 and with the period below the threshold between 2008 and 2013. Subsequently, the below-
353 threshold period continued until August 2016, followed by (1) a spike (426 shrimp m⁻²) in March 2017, which ought to
354 have been derived from a high abundance of recruits to second 0-y cohort in 2016, (2) a rapid drop-off to the near
355 threshold in July 2017, and (3) a low plateau in the summers of 2018 and 2019.

356 There were three population booms in *M. minutus* over the entire period, with peak abundances of 2164, 1165, and
357 3839 worms m⁻² in 2000, 2007, and 2016, respectively. Each high state lasted 2–3 y. One much lower peak occurred in
358 March 2015. Population sizes in the other years were much smaller. The first population boom coincided with the ghost
359 shrimp population's below-threshold (for gastropod recruitment) phase around 2000. The second boom occurred in the
360 shrimp's about- or a little above-threshold phase around 2007, with means of 144–230 shrimp m⁻². The third boom
361 started in the shrimp's below-threshold phase, and the abundance increased precipitously from May 22 to August 2 in
362 2016. This high state continued until 2017, when shrimp densities overshot the threshold value.

363

364 **Distributions of ghost shrimp and worm on Tomioka sandflat**

365 Yearly changes in the distribution of the three species over Transect G on Tomioka sandflat in 2010 and during 2015
366 to 2019 are shown in Fig. 4. Each line depicting the distribution of *N. harmandi* densities during 2015 to 2019 stands for
367 the summer state except for March 2017. Ghost shrimp densities were much lower in August 2010 than in the 2015 to
368 2019. The distributions for the 1979 to 2014 are given in Tamaki and Takeuchi (2016, fig. 13), in which two types of
369 basic patterns are extracted: (1) during 1984 to 1994, when shrimp occurred at high densities over the transect, and
370 stingray (*H. akajei*) pit abundance was much lower (Tamaki et al. 1997, 2020a), shrimp densities decreased gradually
371 from lower to upper shores (pattern-1). This was primarily derived from the gradual decrease in newly-settled shrimp
372 density along that tidal gradient (Tamaki et al. 1997); and (2) during 1995 to 2014, along with the abrupt increase in
373 stingray abundance and spatially different foraging impact on the shrimp population, shrimp densities were higher on
374 the lower and upper than middle shores (pattern-2; Takeuchi and Tamaki 2014; Tamaki et al. 2020a). In this case,
375 stingray foraging pressure was most intense on the mid-shore due to its thinnest sand column for shrimp vertical refuge.

376 In Fig. 4a, pattern-2 above was observed clearly for 2010, 2016, and 2018 and less so for 2015, with positions of the
377 middle zone with lower ghost shrimp densities varying yearly. The distribution in March 2017 was unique in that
378 densities were at quite high levels over the transect. In July of the same year, densities had dropped off markedly,
379 generally higher in the upper 110-m zone than in the lower zone. The distribution in 2019 was similar to that in July
380 2017 in shape. The results of core sampling for shrimp at the five transect stations help depict their distribution pattern
381 by cohorts. On August 3, 2016, the sand columns were thicker on the upper and lower than mid-shores (Fig. 5a), and in
382 total, 13 adult females [1- and 2-y cohorts; 21.1–34.1-mm total length (TL)], 26 adult males (18.1–36.1-mm TL), and
383 36 juveniles (first 0-y cohort; 4.1–12.1-mm TL) were collected. The adult-density distribution over the five stations
384 exhibited a concave profile (pattern-2), with the minimum at Stn 150, whereas juvenile densities were at a much higher
385 level at Stns 270, 210, and 150 than at Stns 90 and 30 (pattern-1 above), with a peak at Stn 150 (Fig. 5b). The range and
386 mean (\pm SD) for (core-based density for all cohorts – density estimated from burrow openings) / (core-based density) at
387 the five stations were –0.45 to 0.44 and 0.08 ± 0.36 . Except for Stn 150, the profiles for these two kinds of densities
388 were similar. The TL-frequency distributions for male and female shrimp from the five stations on May 27, 2017 (each
389 104 and 97 ind.), with normal-distribution curves fitted to 2-y, first 1-y, and second 1-y cohorts, are given in
390 Supplementary material 3. The proportions of the three cohorts in each TL-class of each sex were applied to the total
391 number of shrimp in that class at each station, and the shrimp number of each cohort from both sexes is indicated in Fig.
392 5c. Densities of the combined cohort were about the same between Stn 270 and Stn 150 and increased from Stn 150 to
393 Stn 30. This spatial pattern was derived from the same pattern shared by both first and second 1-y cohorts, which was a
394 stark contrast to the pattern observed for first 0-y cohort on August 3, 2016 (Fig. 5b).

395 *Mesochaetopterus minutus* occurred in the lower half of the transect between Stn 150 and Stn 270 during 2015 to
396 2019 and at much higher densities between Stn 150 and Stn 190 during the population boom from August 2016 to
397 March 2017 (Fig. 4b). In the areally interpolated worm densities in August 2016, a zonal distribution centered on the
398 mid-shore was detected, with the higher densities up to 49300 worms m^{-2} (actual value) in the sheltered area north of
399 Transect G (Figs. 6a and 1c). Worm densities appeared to be negatively correlated with ghost shrimp densities (Fig.
400 6a,b). Pearson's product-moment correlation coefficient for all plot data was significant ($r_p = -0.36$, $n = 55$, $P = 0.008$),

401 whereas Spearman's rank correlation coefficient was marginally insignificant ($r_s = -0.24$, $n = 55$, $P = 0.083$).

402 Mean (\pm SD) above-ground height of worm tubes was 9 ± 4 mm ($n = 20$), and their blotted wet weights (per 300
403 cm^2) in the sediment depth layers of 0–10, 10–15, 15–20, and 20–25 cm were 20.5, 11.2, 1.2, and 0.4 g, respectively.

404

405 **The abundance and distribution of gastropod relative to ghost shrimp and worm on Tomioka sandflat**

406 In Fig. 3c depicting yearly changes in CP (shrimp→gastropod) and CPB (worm→gastropod), (1) data in putative
407 Octobers are given for most CPs up to 2014, (2) CP value for March 2015 is identical to that for 2014, and (3) July or
408 August data are given for CPB. For CP, (1) initial decline from 1979 to 1984, (2) low profile with values <0.1 during
409 1984 to 1996, and (3) rise and fall between 1996 and 2003 largely conformed to the yearly change in ghost shrimp mean
410 density across the threshold for gastropod recruitment success (Fig. 3a). Between 2003 and 2007, the rise-and-fall
411 profile in CP was of a reversed shape of the profile in shrimp density above that threshold. After 2007, the three clumps
412 of CP largely mirrored the change in shrimp density across the threshold. CP values during 2008 to 2013 were much
413 higher than those of the other clumps, and the almost zero in March 2017 was due to the shrimp density spike (Fig. 3a).
414 The profile of CPB through time was the same as that of the worm abundance (Fig. 3b), which reflected the co-
415 occurrence of worm and juvenile gastropods at high densities at the mid-transect stations (Tamaki and Takeuchi 2016).

416 The *U. moniliferum* shell width-frequency distributions during 2015 to 2019, with 0+ old cohort and 1+ and older
417 cohort separated on each occasion, are given in Supplementary material 4 [see Tamaki and Takeuchi (2016, fig. 10) for
418 those distributions during 1979 to 2014]. A 3-y life span was detected from the temporal sequence of cohorts. On
419 Transect G in 2010 and during 2015 to 2019, both 0+ old cohort and 1+ and older cohort occurred from Stn 90 seaward,
420 with the latter distributed largely more seaward (Fig. 4b–k). In Fig. 3d depicting yearly changes in the total number of
421 individuals of 0+ old cohort and that of all (two) cohorts over the transect stations (i.e., the abundances for the transect),
422 the values in July or August are indicated for the 1979 to 2014 (adapted from Tamaki and Takeuchi 2016, fig. 11A),
423 whereas those on all sampling occasions are indicated for the 2015 to 2019. Six possible causal links from CP
424 (shrimp→gastropod) and CPB (worm→gastropod) to the gastropod 0+ old-cohort's abundance are illustrated by
425 arrowed dotted lines from Fig. 3c to Fig. 3d. During 1979 to 1996, the shape for the profile of CP was similar to that of

426 the gastropod abundance in both 0+ old cohort and combined cohort. During 1996 to 2003, CPB profile was inside CP
427 profile, both of which largely corresponded to the profiles of the gastropod abundances. In 2004 and 2005, CP values
428 were reflected in the abundance of combined gastropod cohort to some extent, but not in that of 0+ old cohort. The latter
429 might be due to some sampling error for smaller gastropods. Despite almost zero CP in 2007, a large value of the
430 gastropod 0+ old cohort abundance was recorded in 2008. The sub-peak in CPB in 2008, with abruptly increased CP,
431 was coincident with the local peaks in the abundances of gastropod 0+ old cohort and combined cohort in 2009. During
432 2009 to 2013, despite high CPs, the gastropod 0+ old cohort abundance decreased precipitously. In particular from 2011
433 onward, a low profile continued for the abundances of gastropod, nearing zero in 2019, but with small peaks in the 0+
434 old cohort abundance in the springs of 2015, 2016, and 2017. Particularly noted is the correspondence of that cohort's
435 peak in 2016 to the CP peak and that of the cohort peak in 2017 to both very high CPB peak and (almost) zero CP.

436

437 **Spatial and temporal changes in sediment properties and surface topography on Tomioka sandflat**

438 Distributions of $Md\phi$, σ_1 , and silt-clay content of the surface 1-cm sediment on Transect G of Tomioka sandflat in
439 2010 and during 2015 to 2018 are shown in Fig. 7a–c, for which summer data are given except for March 2017.
440 Between August 2010 and March 2017, the profiles for each of $Md\phi$ and σ_1 were alike in position and shape despite the
441 extremities in ghost shrimp density, lowest in 2010 and highest in 2017 (Fig. 4a). Both parameter values largely
442 increased from lower to upper shores, indicating the shift from (very) well-sorted medium sand to moderately-sorted
443 fine sand. Coarsening, better sorting, and lowering in mud content of the surface sediment over the transect occurred
444 continuously in the course of ghost shrimp population boom, peak, and shrink until 2010, from which onward those
445 parameter values appeared to have reached respective constants at each station regardless of shrimp densities except for
446 plots excavated by stingrays (Tamaki et al. 2018b, fig. 6). Stingray visits are less at locations with lower shrimp
447 densities during late spring to autumn and seasonally least during winter to early spring (Takeuchi and Tamaki 2014;
448 Tamaki et al. 2020a). Regarding the present data set, stingray pit abundances were at the minima in August 2010,
449 associated with the lowest shrimp densities, and in March 2017 (A. Tamaki, S. Takeuchi, and G. Sagara, pers obs). Most
450 $Md\phi$ and σ_1 values in 2015, 2016, July 2017, and 2018 deviated from the closely positioned lines for 2010 and March

451 2017 (circle plots in Fig. 7a,b). This could be caused by different degrees of stingray sediment excavation among these
452 occasions, which was assessed by (1) examining several available data sets of $Md\phi$ and σ_1 for the surface 1-cm and 3-
453 cm sediments at all stations on Transect G and (2) estimating daily reduction rates in ghost shrimp densities from spring
454 to summer, as follows. Figure 8a shows the plots for the mean value, over the transect stations, of the absolute
455 difference in σ_1 between 1-cm and 3-cm sediments at each station versus the mean value of such differences in $Md\phi$.
456 The plots for August 2016 and July 2017 were above those for August 2010, March 2017, and August 2018, and the
457 sequence from August 2016, via March 2017, to July 2017 was downward and upward. This suggests that the increased
458 heterogeneity in the two parameters' values from spring to summer in 2017 was caused by sediment excavation by
459 stingrays. Figure 8b shows the estimated daily shrimp reduction rates at Stns 30, 90, 150, 210, and 270 from March to
460 July (August) in 2010, 2015, and 2017 and from May to August in 2016. That rate was defined as (density in spring –
461 density in summer) / (density in spring \times lapse of days), with negative values plotted as zeroes in the figure. The rate
462 was lowest in 2010, suggesting the least stingray visit under the lowest abundance of shrimp (Fig. 4a). In the other
463 years, the rates were lower at Stns 30 and 90 than at Stns 150, 210, and 270. This is consistent with the greater sediment
464 excavation by stingrays on the lower than upper shores in August 2012 (Takeuchi and Tamaki 2014), providing an
465 interpretation for the higher shrimp reduction rates on the lower-half than upper shores from March to July in 2017.

466 Silt-clay contents of the surface sediment on Transect G were mostly close to or equal to zero (i.e., below the
467 instrumental detection limit) on the lower-half shore and increased from the mid-shore landward (Fig. 7c), indicating
468 part of the tendency of sediment fining in that direction (preceding par.). The long-term reduction in the silt-clay
469 fraction over the transect is attributable to ghost shrimp blowing off of those finest particles (Tamaki et al. 2018b).
470 Some spots with the higher silt-clay contents on the middle shore in 2010 accorded with the lowest shrimp densities
471 there (Fig. 4a). The higher contents on the upper shore in 2016 was in parallel with the higher ground height in 2016
472 than in 2015 and 2017 (Fig. 7d), suggesting the progression of sediment accretion from 2015 to 2016 and erosion from
473 2016 to 2017. These two contrasting sediment changes occurred concurrently with the outbreak of *M. minutus* in 2016
474 (Fig. 4b) and the inferred increase in stingrays' sediment excavation intensity in 2017 (preceding par.), respectively.

475 In six pairs of sediments from the grain mass scraped off *M. minutus* tubes and the 1-cm deep clod at each nearby

476 sandflat collected in the area for the census of worm and ghost shrimp densities in August 2016 (Fig. 6), mean (\pm SD)
477 values for $Md\phi$, σ_1 , and silt-clay content were 1.86 ± 0.04 , 0.47 ± 0.09 , and $0.01 \pm 0.01\%$, respectively in the former
478 and 2.01 ± 0.06 , 0.50 ± 0.07 , and $0.09 \pm 0.04\%$, respectively in the latter. Wilcoxon signed-rank tests detected
479 significant differences in $Md\phi$ and silt-clay content ($T = 0$; $P < 0.05$) but not in σ_1 ($T = 9$; $P > 0.05$). The worm appears to
480 select coarser grains from the ambient sediment to make its tube rigid. This gathering of tube material does not appear
481 to have been large enough to affect those three sedimentary parameter values on the mid-Transect G (Fig. 7a–c).

482 Vane shear strengths of surface sediments on Transect G were higher at 4-cm than at 1-cm depths in August 2015,
483 August 2016, and March 2017 (Fig. 7e). On these occasions, groundwater tables were near the sandflat surface: in 2015,
484 range = -2.5 cm (minus: below surface) to 2.5 cm (plus: overflow above surface) and mean (\pm SD) = 0.6 ± 1.4 cm ($n =$
485 16 stations); in 2016 and 2017, -5 to 10 cm and 7.3 ± 4.7 cm ($n = 14$), and 3 to 10 cm and 6.8 ± 2.6 cm ($n = 15$),
486 respectively. This suggests the absence of suction (= negative pore-water pressure relative to atmospheric pressure) and
487 the dependence of hardness of the sediment solely on its state of packing with constituent particles (Sassa and Watabe
488 2007). Both 4- and 1-cm values were mostly higher in August 2016 and March 2017 than in August 2015. Sediment
489 hardening from 2015 to 2016 was consistent with the increase in silt-clay content and the progression of sediment
490 accretion (Fig. 7c,d). Tamaki et al. (2018b) ascribed the reduction in shear strengths at 4-cm depth from both upper and
491 lower shores toward mid-shore in 2015 to the lowest adult ghost shrimp densities in the latter, for which rotating vane
492 blades was supposed to encounter the least resistivity to destroy shrimp burrows. Vane shear strengths at 1-cm depth
493 corresponding to varying groundwater tables in and out of *M. minutus* aggregations (around the blue circle point in Fig.
494 9b) were at higher levels inside than outside in the groundwater table-adjusted comparison (related to suction; Fig. 7f),
495 indicating the higher degree of particle packing in the surface sediment inside the worm aggregations.

496 In the rectangular area for elevation contours (Fig. 9a,b), with Transect G running quasi-diagonally across it, ground
497 heights varied gradually along the tidal gradient in August 2015, while in August 2016, there were sub-areas with the
498 steeper or gentler shore-normal transitions and increased indentations in isobath especially in the mid-tidal zone. This
499 indicates that heterogeneity in the sandflat surface topography progressed from 2015 to 2016. The isobaths with a
500 higher resolution in part of that area (2016-strip) and in its adjacent 2017-strip (Fig. 9c, left and right panels), both

501 containing the segment from Stn 150 to Stn 170 on Transect G near their right edges, depict the following two features:
502 (1) 2016-strip generally consisted of the seaward elevated and landward depressed halves. If a dome-shaped elevation
503 with a closed isobath on its base is regarded as an ellipsoid in plane aspect, area and height of the three distinct
504 elevations in the seaward half ranged from 27.5 to 42.2 m² and 3 to 8 cm, respectively. Those of the leftmost distinct
505 depression in the landward half was 34.6 m² (ellipsoid) × 5 cm (maximum depth). The maximum depth of the other
506 distinct depression was 5 cm; and (2) 2017-strip generally consisted of the outer depressed and inner elevated parts; the
507 maximum heights of the elevations were 3–5 cm, and the maximum depths of the depressions were 3–6 cm. Normally,
508 the 2017-strip is situated higher than the 2016-strip along the tidal gradient. Despite this, the mostly lower local ground
509 heights in the 2017-strip indicates the greater erosion of its surface from 2016 to 2017, which is consistent with the
510 greater reduction in heights around Stn 150 than around Stn 170 on Transect G during that period (Fig. 7d). The aerial
511 photograph from 32-m height, centered at the blue circle point in Fig. 9b, depicts a mosaic of sub-areas consisting of
512 elevated worm-tube aggregations with few small sand ripples, water-filled depressions including stingray foraging pits
513 (cf., Takeuchi and Tamaki 2014, fig. 2; Tamaki et al. 20020a, fig. 8), and the other parts with clear small ripple arrays
514 (Fig. 9d). The isobaths interpolated for ground heights around one worm aggregation in a 6- × 6-m plot indicate a 7.5-
515 cm maximum height (Fig. 9e for the red square plot in Fig. 9b). Elevated worm aggregations formed in the ghost shrimp
516 bed are less distinct in both whole profile and boundary to the ambient flat part than neat dome-shaped mounds formed
517 under few or no shrimp in the former time (Tamaki and Takeuchi 2016, fig. 14B; Supplementary material 2).

518

519 **Population densities of ghost shrimp and gastropod on eastern Amakusa-Shimoshima Island**

520 The mean (\pm SD) surface burrow-opening density of ghost shrimp on U6 sandflat of A.-S. Island in July 2017 was
521 95.7 ± 84.3 counts m⁻² ($n = 30$ stations), and the value on U7 sandflat in May 2018 was 68.2 ± 63.8 counts m⁻² ($n = 24$).
522 In July 2017, the shell width range and mean density of *U. moniliferum* (gastropods m⁻²; n) per sandflat were 11.2–13.6
523 mm and 3.2 ($n = 30$) on U6, 8.8–13.2 mm and 10.0 ($n = 10$) on U5, 10.8–12.4 mm and 4.3 ($n = 7$) on U3, and nil ($n = 8$)
524 on U2. Those values on U7 sandflat in May 2018 were 5.9–8.5 mm and 2.8 ($n = 24$).

525

526 Retrieved drift cards on Tomioka sandflat at three release sets

527 Of the data on the number of drift cards daily retrieved in and around Tomioka sandflat, only those from the main
528 part of the sandflat was adopted (Fig. 10a, inset, red thick line), as it is the *U. moniliferum*'s habitat area (Tamaki and
529 Takeuchi 2016). Each card-release point on the three occasions in 2008 (Release-1) and 2009 (Releases-2 and -3) and its
530 presumed corresponding set of intertidal sandflat populations on A.-S. Island as a nearby sender of larvae are indicated
531 in the inset maps of Fig. 10a,c. The daily cumulative numbers of cards derived from each release point and the temporal
532 changes in tidal heights for Tomioka Bay [from records by Japan Meteorological Agency for Nagasaki Harbor located
533 30 km north of Tomioka Bay (<https://www.data.jma.go.jp/gmd/kaiyou/db/tide/genbo/genbo.php>); those for around
534 Tomioka Bay available only for July 2010 and afterward; the high- or low-tide time in Tomioka is 5 to 10 min behind
535 that in Nagasaki] and in wind velocities at Tomioka Fishing Harbor [Fig. 10a, inset, red triangle point; data recorded
536 every 10 min by Kumamoto Prefecture Government (download source given in Mandal et al. 2010, sect. 2.2)] are
537 shown in the upper, middle, and lower rows of Fig. 10b,c, respectively. Tamaki et al. (2018a) demonstrated that in
538 Tomioka Bay, the tidal range from high- to low-tide times can be used as a measure for the strength of ebb currents
539 transporting larvae released from Tomioka sandflat toward the coastal ocean. The tidal ranges were almost the same
540 between Release-1 and Release-2 (205 cm and 199 cm) and smaller at Release-3 (68 cm). The mean (\pm SD) speeds of
541 winds from the northeast–northwest directional sector potentially carrying cards ashore or southeast around the time of
542 each release were $4.0 \pm 0.5 \text{ m s}^{-1}$ ($n = 8$), nil, and $4.6 \pm 0.65 \text{ m s}^{-1}$ ($n = 5$) at Releases-1, -2, and -3, respectively.
543 Through the whole card retrieval period each year, northerly winds were prevalent. Largely, their speeds were lower in
544 2008 than in 2009, when their occurrences were more continuous between Release-2 and Release-3 than after Release-3
545 with intermittent higher speeds than in the former period. Following Release-1 made on October 3, 2008 (Day 0),
546 clusters of cards derived from Tomioka Bay were found around 2 km north of Tomioka Headland on Day 1 and around
547 1.2 km north of Tsuji-Shima Island on Day 3 by a local fisherman engaged in the card release (T. Kawamoto, pers
548 comm; see Fig. 1a,b for locations). The retrieved cards came from Tomioka Bay (R1-1; i.e., retention) and the two most
549 distant points (R1-4 and R1-5), first on Day 8 (R1-5) subsequent to the neap tide period (Fig. 10b). The largest
550 cumulative number of cards was from the most distant point. Regarding Release-2, for simplicity, the results for the five

551 release points off the eastern shoreline of A.-S. Island were combined into those for three points (R2-2, R2-3, and R2-4;
552 Fig. 10c). In the first continuous retrieval period from October 15, 2009 (Day 0), low numbers of cards from Tomioka
553 Bay (R2-1; retention), R2-2, and R2-3 were obtained, first on Day 1 for R2-1 and first on Day 3 for R2-2 and R2-3.
554 Over the second and third continuous retrieval periods, the more numbers of cards were of these allochthonous origins,
555 with only a single card from the most distant point (R2-4, close to R1-5). The timing of Release-3 made on October 27,
556 2009 (Day 0) accorded with the presumed actual timing of the gastropod's mass gamete spawning in the neap of
557 spring-neap tidal cycle (Mandal et al. 2010, fig. 8). Of the three card-release sets, the highest degree of card retention in
558 Tomioka Bay was recorded at Release-3, with its value greater for the release point closer to the sandflat than for the
559 seaward point (68% vs. 25.5% cumulative retrieval rates on Day 9). Much fewer cards of the allochthonous origins
560 came first on Day 7 (syzygy), with cumulative retrieval rates of 1.2% on Day 9 and 1.7% on Day 17 for R3-2 and R3-3
561 inclusive. A single card came from the most distant point (R3-4) first on Day 9, with 7 cumulative cards by Day 17.
562 Casual observations on cards stranded on intertidal sandflats other than Tomioka through 2008 and 2009 recorded some
563 retention from R2-4 and R3-4 points to U6 and U7 sandflats and some transport from R3-2 and R3-4 to U5 on Day 4.

564

565 **Discussion**

566 The present study was based on a 40-y monitoring of the benthic community on an intertidal sandflat. The aim was
567 to better understand the complex interplay among a ghost shrimp as a sediment destabilizer, a tube-building polychaete
568 worm as a stabilizer of part of the shrimp bed, and a stingray feeding on the shrimp, as another sediment destabilizer, in
569 affecting the fluctuation of a gastropod population in its regional metapopulation context.

570 The two recovery events from the (near) extinct states of the *U. moniliferum* population on Tomioka sandflat in the
571 2000s (Fig. 3c) indicate the entry of larvae from somewhere else. By applying net reproductive rate (R_0) to the Tomioka
572 population, Tamaki and Takeuchi (2016) demonstrated that even in its high states, the population requires allochthonous
573 larvae to persist (i.e., demographic sink with $R_0 < 1$), with estimated subsidy ratios of allo- to auto-chthonous larvae in
574 three years with data sets for calculation available ranging from 0.7 to 1.6. The present results for the drift card release
575 and retrieval revealed that gastropod larvae can be transported from the eastern shoreline of A.-S. Island to Tomioka

576 sandflat, in particular within the substantial larval surviving duration (9 d) when released around neap tides. Regarding
577 larval dispersal distances of marine benthos, data for 1–20 km are the least (Todd 1998; Shanks 2009). Of the three
578 card-release sets in the present study, data at Release-3 are most suitable for demographic analysis because the release
579 timing (neap tide date) coincided with the actual larval release timing of the spring–neap tidal cycle (Mandal et al.
580 2010) and the daily retrieval was conducted up to Day 9. An estimation was made for the proportional contribution of
581 the cards (as virtual larvae) which reached Tomioka sandflat ‘alive’ from Tomioka itself and that of the cards from each
582 combined population group of the *Un* sandflats in A.-S. Island to all cumulative ‘survivors’ for the period from Day 3
583 (shortest PLD) to Day 9 (see Supplementary material 5 for details). The proportion of the total ‘survivor cards’ from
584 each of the two release points in Tomioka Bay to all ‘survivor cards’ including the ones from the three release points off
585 the *Un* sandflat groups (U1–U3; U4 + U5; U6 + U7) was estimated to be 79.1% and 56.3%, respectively. Among the *Un*
586 groups, the contribution from U6 and U7, farthest from Tomioka sandflat, was smallest (10.5% of all *Uns*). Drift cards
587 or alike have been used to infer dispersal of larvae among benthic habitats (Levin 1983; Scheltema 1986). The present
588 study has presented the first application of such cards to the assessment of a local population as a demographic sink.

589 Other than *U. moniliferum*, two congeneric species exhibited lecithotrophic larval retention in embayments,
590 potentially precluding larval export to the coastal ocean or a large estuary (Berry 1986; Noda and Nakao 1995, 1996).
591 Tamaki and Takeuchi (2016) and Tamaki et al. (2018a) demonstrated that although *U. moniliferum* is a larval retention
592 strategist, full retention in Tomioka Bay is not realized because of its location close to the coastal ocean with strong tidal
593 currents entraining larvae. The high likelihood of gastropod larval supply from the eastern shoreline of A.-S. Island to
594 Tomioka sandflat may be understood from Strathmann et al.’s (2002) viewpoint that part of larvae leaking from their
595 return-home loop in a self-sustaining local population could help sink local populations persist. In Penang, Malaysia, a
596 local population of *U. vestiarius* went extinct but later recovered with allochthonous larvae (Ong and Krishnan 1995).

597 Of the *U. moniliferum* populations on the *Un* sandflats of A.-S. Island, those on U6 and U7 are most likely to be the
598 main demographic source for the other *Un* populations in light of the largest sizes of the former situated farthest from
599 Hayasaki Straits (Fig. 1d) and of the weakest tidal currents around them (Fujiie et al. 2006), enabling the highest degree
600 of larval retention. U5 population may be second to this in source status. U1–U4 populations may not necessarily

601 sustain themselves because of weaker shoreline concaveness allowing for poor larval retention in each inconspicuous
602 embayment and of their positions closer to the coastal ocean, with greater degrees of larval export (cf., Tamaki et al.
603 2020b). The time taken for larval transport from a U_n sandflat toward Hayasaki Straits would primarily be governed by
604 ebb tidal current speed, which is positively related with tidal range and negatively with the distance to the straits. In
605 October 2009, when cards were released around or a few days after the quadrature, those from off U1–U4 (and U5)
606 were retrieved more than from off U6 and U7 on a time scale of the substantial gastropod PLD (Fig. 10). The continuity
607 (after Release-2) or intermittence (after Release-3) of northerly winds while cards were supposed to be in the coastal
608 ocean provides one explanation for the difference in the speeds with which they reached Tomioka sandflat between the
609 two releases. U1–U4 populations would act as an effective sender of larvae to the Tomioka population situated at the
610 westernmost position, whereas U6 and U7 (and U5) populations may not. Therefore, U1–U4 populations could act as
611 stepping stones, receiving larvae from the U5–U7 and sending larvae further north by their descendants. This view
612 raises caution that a demographic source–sink relationship should be distinguished from the larval sender–receiver
613 relationship when a specific receiver population (e.g., Tomioka) is destined for as a demographic sink. In October 2008,
614 when cards were released a few days after the syzygy (Release-1), those from off U1–U3 never reached Tomioka
615 sandflat, whereas those off U6 and U7 were most abundant and those from Tomioka Bay the second, all occurring only
616 after the substantial gastropod PLD. Such a situation with U1–U3 illustrates a setting for larval export strategists,
617 including *N. harmandi*, utilizing stronger ebb tidal currents to rapidly separate newly-hatched larvae away from the
618 adult habitat. Cards from off U6 and U7 might be given some time to reach Hayasaki Straits around the ensuing neap
619 tide with weaker tidal currents retaining them near Tomioka Bay. The longer time for cards to arrive at Tomioka sandflat
620 in 2008 than in 2009 might be due to the weaker northerly winds in 2008. The present drift card results point to the
621 importance of larval release timing in season, tidal cycle, and weather for the realized connectivity of local benthic
622 populations in a specific shoreline configuration with its nearshore waters setting (Carson et al. 2010; McQuaid 2010).

623 Although the conditions of both high CPs (shrimp→gastropod) and high CPBs (worm→gastropod) on Tomioka
624 sandflat in 2016 were similar to those in 2000 and 2005–2007 owing to both low *N. harmandi* densities below the
625 threshold inhibiting gastropod recruitment ($160 \text{ shrimp m}^{-2}$) and outbreaks of *M. minutus*, the abundance of *U.*

626 *moniliferum* was at a much lower level around 2016 than in those previous years (Fig. 3). Already from 2011, the
627 gastropod had exhibited no signs of recovery despite the high levels of CP. The primary cause for this would be the
628 recent nearly extinct state of the main gastropod populations on the *Un* sandflats of A.-S. Island (U5–U7; fifth sub-sec.
629 of the Results). The present regional metapopulation might be approaching a demise. The reason for the decline of U6
630 and U7 populations is unknown. At least, ghost shrimp densities remained as low as in 1998. Recently intensified wet-
631 monsoonal rainfall brings about acute riverine mud deposition on these sandflats (Fig. 1d for river locations), which
632 could suffocate epibenthic filter-feeding molluscs (A. Tamaki, Y. Sogawa, and H. Ohashi, pers obs). Freshwater runoff
633 was regarded as a cause for a temporary extinction of a local population of *U. vestiarium* (see Ong and Krishnan 1995).

634 The two intermittent outbreaks of *M. minutus* on Tomioka sandflat in the 2000s occurred concurrently with those on
635 several intertidal sandflats of the region (A. Tamaki, Y. Sogawa, and H. Ohashi, pers obs). PLD of *M. sagittarius* is
636 suggested to last several months, during which larvae could be transported long distances [Bhaud et al. (2002); see
637 Scheltema (1986) for chaetopteric teleplanic larvae]. For populations of *Mesochaetopterus*, settling larvae may come
638 from too far away for their origins to be inferred. On Tomioka sandflat, the inhibitory effect of *N. harmandi* on the
639 recruitment of *M. minutus* is obvious from spatially and temporally negative correlations between their densities
640 (Supplementary material 2; Figs. 3 and 6). One outbreak on Tomioka sandflat occurred in 1978 (T. Kikuchi, pers
641 comm), conducive to the 1979 abundance (Tamaki and Kikuchi 1983; Supplementary material 2). It was not until
642 around 2000 that any subsequent outbreak occurred, when the ghost shrimp population had been run down (Tamaki et
643 al. 2020a). The empirical threshold *N. harmandi* density for inhibiting *M. minutus* recruitment seems to be common to
644 or a little higher than that for *U. moniliferum* recruitment (160 shrimp m⁻²; Fig. 3). Ghost shrimp are known to inhibit
645 the recruitment of small tube builders (Tamaki 1985; Posey 1986; Wynberg and Branch 1994; Berkenbusch et al. 2000;
646 Pillay et al. 2007a). At its adult stage, however, the *M. minutus* population withstood the higher densities of *N.*
647 *harmandi*, as observed in 2007 and March 2017 (Figs. 2 and 3); the high shrimp density in 2017 was from the boom of
648 recruits the previous late summer to autumn (Figs. 3–5), and that high state was widespread on shores of the regional
649 coastal ocean (A. Tamaki and S. Takeuchi, pers obs). The resistivity of aggregated adult worms to ghost shrimp may
650 come from their tubes' relatively rigid structure and long subsurface reach (to a depth of 15 cm) potentially interfering

651 with shrimp burrow construction; see Tamaki et al. (2018b, fig. 2) for casts of burrow clusters and Tamaki et al. (2020a,
652 fig. 3) for the vertical distribution of juvenile shrimp, with TL \leq 10 mm to 10-cm depth, sub-adults with 10 to 20-mm TL
653 to 15 cm, and adults to the sand column bottom. Softer and shorter tubes of infauna like spionid polychaetes could not
654 serve as such a barrier. On Tomioka sandflat, worm aggregations seemed to facilitate ghost shrimp postlarval settlement
655 (Fig. 5b) but later to make grown shrimp (old juveniles to young sub-adults) emigrate landward (Fig. 5c); migration of
656 *N. harmandi* juveniles is common (Tamaki and Ingole 1993; Tamaki et al. 2013). The worm tubes' protection of shrimp
657 settlers from predation, followed by their competition for space with larger shrimp (Brenchley 1982), might be involved
658 there. The weak negative correlation between the densities of worm and ghost shrimp of all cohorts around the mid-tidal
659 zone of the sandflat also implies competition for space (Fig. 6), though stingray (*H. akajei*) predation on shrimp (Fig. 9)
660 could blur this relationship. The increased sediment hardness induced by worm tube aggregations may have suppressed
661 re-burrowing of grown shrimp despite their enhanced burrowing capability compared with that of smaller shrimp; see
662 Sassa and Yang (2019, figs. 5 and 6) for results of a laboratory experiment using a congeneric ghost shrimp, *N.*
663 *japonica*. There is an additional possibility that three processes listed below led to the emigration of expelled (to the
664 sandflat surface) but surviving juvenile shrimp from lower-half toward upper shores: (1) shrimp density-dependent
665 foraging by stingrays (Takeuchi and Tamaki 2014); (2) medium to large rays' preference to the lower shore (Takeuchi
666 and Tamaki 2014); and (3) escape of juvenile shrimp from rays' shrimp size-selective predation (Tamaki et al. 2020a).

667 The deep burrow-dwelling polychaete, *Arenicola marina*, and the rigid tube-building polychaete, *Lanice conchilega*,
668 inhabiting tidal flats fringing the North Sea, Europe are regarded as the topmost sediment-destabilizing and -stabilizing
669 ecosystem engineers, respectively (Flach 1992; Reise 2002; Callaway et al. 2010; Alves et al. 2017). When *A. marina*
670 was excluded from large field experimental plots, *L. conchilega* attained much higher densities than at intact plots
671 through increased recruitment (Volkenborn and Reise 2007). Although Volkenborn et al. (2009) mentioned the
672 possibility of natural exclusion of *A. marina* by *L. conchilega*, there are no reports demonstrating this at population
673 levels. The other cases for the exclusion of arenicolid polychaetes by tube builders were via sediment consolidation by a
674 corophiid amphipod (Reise 1978: field expt.) and predation of juveniles by spionid polychaetes [Reise (1978: field and
675 laboratory expts.); Wilson (1981: lab. expt.)]. The record for *M. minutus* and *N. harmandi* in the present study is the first

676 to suggest any counteracting effect of a tube builder aggregation on a large infaunal sediment destabilizer assemblage.

677 After the whole Tomioka sandflat was occupied by *N. harmandi* in 1984, the relief of individual *M. minutus*
678 aggregations became less distinct than that of neat dome-shaped mounds formed seaward of the upper ghost shrimp
679 zone in 1979 [Figs. 2 and 9; Supplementary material 2; Tamaki and Takeuchi (2016, fig. 14B)]. Where sandflat surface
680 sediments are continuously mixed with loosely packed sediments expelled by ghost shrimp (Posey 1986; Dittmann
681 1996; Berkenbusch et al. 2000; Pillay et al. 2007b; Tamaki et al. 2018b) or by stingray, they are more easily dispersed
682 by water flows than firmly packed sediment (Tamaki et al. 2020a), probably with less concentration of sediment
683 particles around tubes. The values on highest *M. minutus* density and maximum height of worm aggregations are
684 comparable to those for mounds made by *M. sagittarius* and another chaetopterid polychaete, *Phyllochaetopterus*
685 *verrilli*, in a wave-swept fringing reef flat in Hawaii (Bailey-Brock 1979). There, the threshold worm density to form
686 mounds was 11000 worms m⁻², with the maximum mound height of 7–10 cm, and a greater proportion of fine sand
687 (0.25–0.063 mm) was present within the mounds as compared with the adjacent areas where coarser materials (0.5–7.9
688 mm) predominated. On Tomioka sandflat, in a more sheltered setting, both median grain size and sorting coefficient of
689 the surface sediment with *M. minutus* aggregations in the mid-segment of the shore-normal transect were similar to
690 those in the nearby segments (Fig. 7a,b). By contrast, the increase in sediment silt-clay content in the middle to upper
691 shore and the elevated ground height in the middle to lower shore were conspicuous (Figs. 7c,d). The progression of
692 elevation–depression arrangements over a wider area of the sandflat from 2015 to 2016 (Fig. 9a,b) suggests that the
693 change in ground height induced by worm aggregations in the mid-tidal zone (Figs. 6 and Fig. 9c, left) ought to be
694 transmitted toward both higher and lower zones. The extended change in landscape-scale relief and the increase in
695 sediment mud content associated with a local patchwork of tube aggregations have been recorded most intensively for
696 *L. conchilega* populations on tidal flats of the North Sea and adjacent waters [relief : Carey (1987), Callaway (2010),
697 Borsje et al. (2014); mud content: De Smet (2015), Alves et al. (2017)]. Density-dependent predation on benthic prey by
698 fish, bird, and large invertebrates with exoskeleton can accentuate substrate topographic changes when they are strong
699 sediment excavators. On Tomioka sandflat, scattering of sediment median grain size and sorting values (Fig. 7a,b) and
700 the increased surface erosion (Figs. 7d and 9c) could consistently be interpreted by the presumed increase in stingray pit

701 formation in response to the higher ghost shrimp densities (Figs. 5, 6, 8, and 9). Individuals of *M. minutus* were
702 removed by stingray foraging as its side effect, because almost only ghost shrimp, not the worm, were found in the fish
703 guts collected at the worm population boom in 2000 (Tamaki et al. 2020a). It is uncertain whether this shortened the
704 worm population durability. Such an incidental destruction of tube aggregations with subsequent topographic changes
705 was reported for eider duck foraging on mussel spat attached to *L. conchilega* tubes on a tidal sandflat (Carey 1987).
706 Sediment digging by rays to directly forage on a tube-building oweniid polychaete was regarded as a main agent that
707 crushed its dense beds on a shallow subtidal sand (Fager 1964). Intensive feeding by migratory shorebirds on a dense
708 bed of a tube-dwelling corophiid amphipod resulted in increased sediment erosion on a tidal flat (Daborn et al. 1993).
709 Tube stands of adults of an onuphid polychaete provide a refuge for infauna preyed upon by portunid and horseshoe
710 crabs digging pits on a tidal sandflat, though juvenile onuphids could be reduced by these predators (Woodin 1981).

711 In the 2000s on Tomioka sandflat, the peaks in the density of 0+ old cohort of *U. moniliferum* occurred in the same
712 year as for the first *M. minutus* population boom or 1 y after its second boom (Fig. 3b–d). After 2015, though low in
713 their heights, peaks in 0+ old gastropod density took place in the spring of 2016 and 2017, suggesting that at least
714 autochthonous recruitment should have been boosted by the third worm outbreak and permitted by the lower *N.*
715 *harmandi* densities. Particularly noted is the possible positive influence by the worm overwhelming the potentially large
716 negative one by ghost shrimp in the autumn of 2016 (reflected in CPB and CP values for March 2017), which is similar
717 to the situation in the autumn of 2006 (reflected in August 2007). Such a worm effect on gastropod recruitment might be
718 greater in the midst of the ghost shrimp bed rather than in the shrimp-free zone (Supplementary material 2), because
719 worm aggregations in the former were more or less continuous over the mid-tidal zone (Fig. 6) as a result of the more
720 dispersibility of loosely packed sediment particles, compared with island-like worm mound distributions in the latter.

721 Two possible mechanisms by which recruitment of small-sized infauna is inhibited by ghost shrimp bioturbation
722 have been proposed: (1) interference with filter-feeding of mollusc juveniles with resuspended sediment load or their
723 spat burial underneath loosely packed sediment (Tamaki 1994; Dittmann 1996; Berkenbusch et al. 2000; Feldman et al.
724 2000; Dumbauld et al. 2006); and (2) hindrance to tube building of juveniles or their burial (Brenchley 1981; Tamaki
725 1985; Posey 1986, 1987). Joint field and laboratory experimental approaches to these mechanisms are limited to

726 Murphy (1985) and Pillay et al. (2007b) in support for the above (1). In addition, regarding the scarcer abundances of
727 juveniles of a filter-feeding mollusc and tube-building infaunas in a natural ghost shrimp bed and a field shrimp-
728 exclusion plot than in the respective control plots, Pillay et al. (2007a) demonstrated significantly lower abundances of
729 benthic microalgae (BM) and extracellular polymeric substance (EPS) in sediments of the former plot. The authors
730 proposed that the poorly developed BM and EPS film on the surface of the loosely packed sediment created by shrimp
731 bioturbation could cause increased resuspension of both sediment particles and juveniles into the water column,
732 conducive to the exclusion of the latter. It is now well established that the sediment of infaunal tube aggregations owes
733 its stability to a complex film of bacteria, BM, and their exudates binding mineral and biogenic inorganic particles
734 (Eckman et al. 1981; Eckman 1985; Passarelli et al. 2014; Alves et al. 2017). Both these particles and benthic juveniles
735 can be prevented from resuspension by that film (Paterson and Hagerthey 2001). On Tomioka sandflat, newly-settled *U.*
736 *moniliferum* juveniles (0.2 mm in size) attach to coarser sand grains (A. Tamaki and S. Mandal, unpubl data), which can
737 easily be resuspended by water flows in high-density *N. harmandi* assemblages and swept away. This process may not
738 have worked efficiently in the mid-tidal zone with *M. minutus* aggregations, which was the central zone for gastropod
739 recruitment (Tamaki 1994). The absence and presence of small ripples on the sandflat surface with worm aggregations
740 and its outside area, respectively (Fig. 9d) suggest reduced sediment resuspension in the former. Disappearance of ripple
741 marks is recognized as a sign of sediment surface stabilization in benthic tube mats (Fager 1964; Bolam and Fernandes
742 2003). The higher hardness of the surface 1-cm sediment associated with worm tube aggregations in 2016 than in the
743 outside and in 2015 (Fig. 7e,f), together with the more elevated shore-normal transect relief in 2016 (Fig. 7d), suggests
744 enhanced sediment particle packing. In addition, increased silt-clay particles (Fig. 7c) would bind coarser particles to
745 strengthen sediment cohesiveness, which could contribute to reducing sediment resuspension. On the aforementioned
746 intertidal sandflat in Penang, sediment stabilization by the increased abundance of a tube-building onuphid polychaete
747 took place prior to the restoration of *U. vestiarium* population (Ong and Krishnan 1995). Other possible mechanisms for
748 increased mollusc juveniles around tube aggregations include (1) passive accumulation of settling larvae with water
749 flow attenuation close to the sediment surface (Armonies and Hellwig-Armonies 1992; Bolam and Fernandes 2003;
750 Mackenzie et al. 2006) and (2) mechanical trapping of drifted juveniles with protruding tubes (Cummings et al. 1996;

751 Volkenborn et al. 2009). In Tomioka, *U. moniliferum* juveniles are carried landward from mid-shore by northerly wind-
752 induced waves during autumn to winter and return seaward by floating on ebb tidal currents in spring (Tamaki 1987;
753 Mandal et al. 2010; Tamaki and Takeuchi 2016), which might be caught with worm tube stands. Varying wind velocities
754 and juvenile movement distances would be reflected in yearly variations in the 0+ old cohort distribution (Fig. 4c–k).

755 It now appears to be a general rule for tidal flat macrobenthos that populations of large infaunal sediment
756 destabilizers, such as ghost shrimp and arenicolid polychaetes, are persistent and those of tube builders, as sediment
757 stabilizers, are more or less ephemeral, being amenable to disturbances from destabilizers, predators with sediment
758 excavation, and storms (Reise 2002; Tamaki and Takeuchi 2016). Those sediment destabilizers may well be recognized
759 as an autogenic and/or allogenic ecosystem engineer (Jones et al. 1994; Berkenbusch and Rowden 2003; Bouma et al.
760 2009; Pillay and Branch 2011), whereas research is underway regarding to what degrees ecosystem engineer status
761 could be assigned to tube builder assemblages on varying spatial and time scales (Berke 2010; Callaway et al. 2010;
762 Rigolet et al. 2014; Alves et al. 2017). The present study system is unique in that a tube-building polychaete population
763 established itself transiently in the midst of a sediment-destabilizing ghost shrimp bed as a knock-on effect of stingray
764 activities with a dual role of predation on shrimp and sediment erosion. One further knock-on step associated with the
765 worm population booms most likely boosted the intermittent recoveries of an epibenthic filter-feeding gastropod.
766 Finally, this local gastropod population change was broadly understood in its metapopulation context.

767

768 **Acknowledgements** We thank staffs of Reihoku Town Office and Fisheries Association for allowing for aerial survey, T. Kawamoto,
769 Y. Agata, Y. Takahara, S. Mandal, and S. Sen-ju for drift card practices, K. Watanabe and S. Goto for ground-height measurement, G.
770 Sagara, H. Ohashi, S. Matsushita, Y. Sato, H. Kamoda, M. Kawata, Y. Matsuda, K. Honma, K. Matsumoto, and K. Ishii for benthos
771 sampling and laboratory works, and T. Takikawa, two reviewers, and handling editor for constructive comments on the manuscript.
772 The water-depth data (Fig. 1a) were provided by Hydrographic and Oceanographic Department, Japan Coast Guard.

773

774 **Funding** This study was partly supported by the Japan Society for the Promotion of Science Grants-in-Aid for Scientific Research
775 KAKENHI JP19310148 and JP26440244 to AT and JP15H02265 to SS.

776

777 **Compliance with ethical standards**

778 **Conflict of interest** The authors declare that they have no conflict of interest.

779 **Ethical approval** All applicable international, and/or institutional guidelines for the care and use of animals were followed.

780

781 **References**

782 Alves RMS, Vanaverbeke J, Bouma TJ, Guarini J-M, Vincx M, Van Colen C (2017) Effects of temporal fluctuation in
783 population processes of intertidal *Lanice conchilega* (Pallas, 1766) aggregations on its ecosystem engineering.

784 Estuar Coast Shelf Sci 188:88–98

785 Armonies W, Hellwig-Armonies M (1992) Passive settlement of *Macoma balthica* spat on tidal flats of the Wadden Sea
786 and subsequent migration of juveniles. Neth J Sea Res 29:371–378

787 Bailey-Brock JH (1979) Sediment trapping by chaetopterid polychaetes on a Hawaiian fringing reef. J Mar Res

788 37:643–656

789 Berke SK (2010) Functional groups of ecosystem engineers: a proposed classification with comments on current issues.

790 Integr Comp Biol 50:147–157

791 Berkenbusch K, Rowden AA (2003) Ecosystem engineering – moving away from ‘just-so’ stories. New Zeal J Ecol

792 27:67–73

793 Berkenbusch K, Rowden AA, Probert PK (2000) Temporal and spatial variation in macrofauna community composition
794 imposed by ghost shrimp *Callinassa filholi* bioturbation. Mar Ecol Prog Ser 192:249–257

795 Berry AJ (1986) Daily, tidal, and two-weekly spawning periodicity and brief pelagic dispersal in the tropical intertidal

796 gastropod *Umbonium vestiarium* (L.). J Exp Mar Biol Ecol 95:211–223

797 Bhaud MR (2005) Evidence of a geographical variation in *Mesochaetopterus* (Polychaeta: Chaetopteridae) from the

798 Pacific Ocean. J Mar Biol Assoc UK 85:1409–1423

799 Bhaud MR, Ravara AA, Macano G, Moreira MH (2002) *Mesochaetopterus sagittarius*: an example of a biogeography

800 discrepancy between larval and adult boundaries: implication for recruitment studies. J Mar Biol Assoc UK

801 82:565–572

802 Biseswar R, Moodley GK, Naidoo AD (2002) Note on an invasion of intertidal zoanthid colonies by a chaetopterid
803 polychaete at Park Rynie Beach, Kwazul-Natal, South Africa. *S Afr J Mar Sci* 24:371–374

804 Bolam SG, Fernandes TF (2003) Dense aggregations of *Pygospio elegans* (Claparède): effect on macrofaunal
805 community structure and sediments. *J Sea Res* 49:171–185

806 Borsje BW, Bouma TJ, Rabaut M, Herman PMJ, Hulscher SJMH (2014) Formation and erosion of
807 biogeomorphological structures: A model study on the tube-building polychaete *Lanice conchilega*. *Limnol*
808 *Oceanogr* 59:1297–1309

809 Bouma TJ, Olenin S, Reise K, Ysebaert T (2009) Ecosystem engineering and biodiversity in coastal sediments: posing
810 hypotheses. *Helgol Mar Res* 63:95–106

811 Brenchley GA (1981) Disturbance and community structure: an experimental study of bioturbation in marine soft-
812 bottom environments. *J Mar Res* 39:767–790

813 Brenchley GA (1982) Mechanisms of spatial competition in marine soft-bottom communities. *J Exp Mar Biol Ecol*
814 60:17–33

815 Buchanan JB, Kain JM (1971) Measurement of the physical and chemical environment. In: Holme NA, McIntyre AD
816 (eds) *Methods for the study of marine benthos*. Blackwell, Oxford, pp 30–58

817 Callaway R, Desroy N, Dubois SF, Fournier J, Frost M, Godet L, Hendrick VJ, Rabaut M (2010) Ephemeral bio-
818 engineers or reef-building polychaetes: how stable are aggregations of the tube worm *Lanice conchilega* (Pallas,
819 1766)? *Integr Comp Biol* 50:237–250

820 Carey DA (1987) Sedimentological effects and palaeoecological implications of the tube-building polychaete *Lanice*
821 *conchilega* Pallas. *Sedimentology* 34:49–66

822 Carson HS, López-Duarte PC, Rasmussen L, Wang D, Levin LA (2010) Reproductive timing alters population
823 connectivity in marine metapopulations. *Curr Biol* 20:1926–1931

824 Cummings VJ, Pridmore RD, Thrush SF, Hewitt JE (1996) Effect of the spionid polychaete *Boccardia syrtis* on the
825 distribution and survival of juvenile *Macomona liliana* (Bivalvia: Tellinacea). *Mar Biol* 126:91–98

826 Daborn GR, Amos CL, Brylinsky M, Christian H, Drapeau G, Faas RW, Grant J, Long B, Paterson DM, Perillo GMF,
827 Piccolo MC (1993) An ecological cascade effect: Migratory birds affect stability of intertidal sediments. *Limnol*
828 *Oceanogr* 38:225–231

829 De Smet B, D’Hondt A-S, Verhelst P, Fournier J, Godet L, Desroy N, Rabaut M, Vincx M, Vanaverbeke J (2015)
830 Biogenic reefs affect multiple components of intertidal soft-bottom benthic assemblages: the *Lanice conchilega* case
831 study. *Estuar Coast Shelf Sci* 152:44–55

832 Dittmann S (1996) Effects of macrobenthic burrows on infaunal communities in tropical tidal flats. *Mar Ecol Prog Ser*
833 134:119–130

834 Dumbauld BR, Booth S, Cheney D, Suhrbier A, Beltran H (2006) An integrated pest management program for
835 burrowing shrimp control in oyster aquaculture. *Aquaculture* 261:976–992

836 Eckman JE (1985) Flow disruption by an animal-tube mimic affects sediment bacterial colonization. *J Mar Res*
837 43:419–435

838 Eckman JE, Nowell ARM, Jumars PA (1981) Sediment destabilization by animal tubes. *J Mar Res* 39:361–374

839 Everett RA (1991) Intertidal distribution of infauna in a central California lagoon: the role of seasonal blooms of
840 macroalgae. *J Exp Mar Biol Ecol* 150:223–247

841 Fager EW (1964) Marine sediments: effects of a tube-building polychaete. *Science* 143:356–359

842 Feldman KL, Dumbauld BR, DeWitt TH, Doty DC (2000) Oysters, crabs, and burrowing shrimp: review of an
843 environmental conflict over aquatic resources and pesticide use in Washington State’s (USA) coastal estuaries.
844 *Estuaries* 23:141–176

845 Flach EC (1992) Disturbance of benthic infauna by sediment-reworking activities of the lugworm *Arenicola marina*.
846 *Neth J Sea Res* 30:81–89

847 Flach E, Tamaki A (2001) Competitive bioturbators on intertidal sandflats in the European Wadden Sea and Ariake
848 Sound in Japan. In: Reise K (ed) *Ecological studies*, vol 151. Ecological comparisons of sedimentary shores.
849 Springer, Berlin, pp 149–171

850 Fujii W, Yanagi T, Tamaki A (2006) Numerical simulation for larval connection network of the ghost shrimp

851 *Nihonotrypaea harmandi* population among intertidal sandflats in Tachibana Bay and Ariake Sound, western
852 Kyushu, Japan. *Mer (Paris)* 44:67–84

853 Fujimoto M (1990) On the characteristics of tides in the Ariake Sea. *J Agricul Engineer Soc, Japan* 58:45–50 (in
854 Japanese)

855 Fukushima S (2006) Fundamental investigation for the advanced trajectory prediction about leeway and divergence.
856 Report of Hydrographic and Oceanographic Researches, Japan Coast Guard 24:107–115 (in Japanese)

857 Gallagher ED, Jumars PA, Trueblood DD (1983) Facilitation of soft-bottom benthic succession by tube builders.
858 *Ecology* 64:1200–1216

859 Hanekom N, Russell IA (2015) Temporal changes in the macrobenthos of sandprawn (*Callianassa kraussi*) beds in
860 Swartvlei Estuary, South Africa. *Afr Zool* 50:41–51

861 Heino J, Melo AS, Siqueira T, Soinenen J, Valenko S, Bini LM (2015) Metacommunity organization, spatial extent and
862 dispersal in aquatic systems: patterns, processes and prospects. *Freshw Biol* 60:845–869

863 Jones CG, Lawton JH, Shachak M (1994) Organisms as ecosystem engineers. *Oikos* 69:373–386

864 Levin LA (1983) Drift tube studies of bay-ocean water exchange and implications for larval dispersal. *Estuaries*
865 6:364–371

866 Mackenzie CL Jr, Pikanowski R, McMillan DG (2006) *Ampelisca* amphipod tube mats may enhance abundance of
867 northern quahogs *Mercenaria mercenaria* in muddy sediments. *J Shellfish Res* 25:841–847

868 Mandal S, Tamaki A, Ohashi S, Takeuchi S, Agata Y, Takahara Y, Harada K, Yamada F (2010) How newly recruited
869 cohorts are formed in the trochid gastropod population (*Umbonium moniliferum*) on an intertidal sandflat in western
870 Kyushu, Japan. *J Exp Mar Biol Ecol* 389:18–37

871 McQuaid CD (2010) Marine connectivity: timing is everything. *Curr Biol* 20(21): PR938–R940

872 Mills EL (1967) The biology of an ampeliscid amphipod crustacean sibling species pair. *J Fish Res Bd Canada*
873 24:305–355

874 Murphy RC (1985) Factors affecting the distribution of the introduced bivalve, *Mercenaria mercenaria*, in a California
875 lagoon—The importance of bioturbation. *J Mar Res* 43:673–692

876 Noda T, Nakao S (1995) Spatio-temporal population dynamics of the sand snail *Umbonium costatum*: importance of
877 ontogenetic migration and annual recruitment variability. *Mar Biol* 123:815–820

878 Noda T, Nakao S (1996) Dynamics of an entire population of the subtidal snail *Umbonium costatum*: the importance of
879 annual recruitment fluctuation. *J Anim Ecol* 65:196–204

880 Ong B, Krishnan S (1995) Changes in the macrobenthos community of a sand flat after erosion. *Estuar Coast Shelf Sci*
881 40:21–33

882 Passarelli C, Olivier F, Paterson DM, Meziane T, Hubas C (2014) Organisms as cooperative ecosystem engineers in
883 intertidal flats. *J Sea Res* 92:92–101

884 Paterson DM, Hagerthey SE (2001) Microphytobenthos in contrasting coastal ecosystems: biology and dynamics. In:
885 Reise K (ed) *Ecological studies*, vol 151. *Ecological comparisons of sedimentary shores*. Springer, Berlin, pp
886 105–125

887 Pillay D, Branch GM (2011) Bioengineering effects of burrowing thalassinidean shrimps on marine soft-bottom
888 ecosystems. *Oceanogr Mar Biol Annu Rev* 49:137–192

889 Pillay D, Branch GM, Forbes AT (2007a) Effects of *Callianassa kraussi* on microbial biofilms and recruitment of
890 macrofauna: a novel hypothesis for adult–juvenile interactions. *Mar Ecol Prog Ser* 347:1–14

891 Pillay D, Branch GM, Forbes AT (2007b) The influence of bioturbation by the sandprawn *Callianassa kraussi* on
892 feeding and survival of the bivalve *Eumarcia paupercula* and the gastropod *Nassarius kraussianus*. *J Exp Mar Biol*
893 *Ecol* 344:1–9

894 Poore GCB, Dworschak PC, Robles R, Mantelatto FL, Felder DL (2019) A new classification of Callianassidae and
895 related families (Crustacea: Decapoda: Axiidea) derived from a molecular phylogeny with morphological support.
896 *Mem Muse Victoria* 78:73–146

897 Posey MH (1986) Changes in a benthic community associated with dense beds of a burrowing deposit feeder,
898 *Callianassa californiensis*. *Mar Ecol Prog Ser* 31:15–22

899 Posey MH (1987) Influence of relative mobilities on the composition of benthic communities. *Mar Ecol Prog Ser*
900 39:99–104

901 R Core Team (2015) R: a language and environment for statistical computing. R Foundation for Statistical Computing,
902 Vienna, Austria. Retrieved from <https://www.R-project.org/>. Accessed July 10, 2020

903 Reise K (1978) Experiments on epibenthic predation in the Wadden Sea. *Helgoländer Meeresunters* 31:55–101

904 Reise K (2002) Sediment mediated species interactions in coastal waters. *J Sea Res* 48:127–141

905 Rhoads DC (1974) Organism-sediment relations on the muddy sea floor. *Oceanogr Mar Biol Annu Rev* 12:263–300

906 Riddle MJ (1988) Cyclone and bioturbation effects on sediments from coral reef lagoons. *Estuar Coast Shelf Sci*
907 27:687–695

908 Rigolet C, Dubois SF, Thiébaud E (2014) Benthic control freaks: Effects of the tubicolous amphipod *Haploops nira* on
909 the specific diversity and functional structure of benthic communities. *J Sea Res* 85:413–427

910 Sassa S, Watabe Y (2007) Role of suction dynamics in evolution of intertidal sandy flats: field evidence, experiments,
911 and theoretical model. *J Geophys Res* 112:F01003

912 Sassa S, Yang S (2019) Role of geoenvironmental dynamics in the biodiversity of sandy beaches and sandflats: The
913 ecohabitat chart and its ecological implications. *Estuar Coast Shelf Sci* 219:278–290

914 Sassa S, Watabe Y, Yang S, Kuwae T (2011) Burrowing criteria and burrowing mode adjustment in bivalves to varying
915 geoenvironmental conditions in intertidal flats and beaches. *PLoS One* 6:e25041

916 Scheltema RS (1986) Long-distance dispersal by planktonic larvae of shoal water benthic invertebrates along central
917 Pacific islands. *Bull Mar Sci* 39:241–256

918 Shanks AL (2009) Pelagic larval duration and dispersal distance revisited. *Biol Bull* 216:373–385

919 Strathmann, RR, Hughes TP, Kuris AM, Lindeman KC, Morgan SG, Pandolfi JM, Warner RR (2002) Evolution of local
920 recruitment and its consequences for marine populations. *Bull Mar Sci* 70(1) SUPPL:377–396

921 Takeuchi S, Tamaki A (2014) Assessment of benthic disturbance associated with stingray foraging for ghost shrimp by
922 aerial survey over an intertidal sandflat. *Cont Shelf Res* 84:139–157

923 Takeuchi S, Takahara Y, Agata Y, Nasuda J, Yamada F, Tamaki A (2013) Response of suspension-feeding clams to
924 natural removal of bioturbating shrimp on a large estuarine intertidal sandflat in western Kyushu, Japan. *J Exp Mar*
925 *Biol Ecol* 448:308–320

- 926 Tamaki A (1985) Inhibition of larval recruitment of *Armandia* sp. (Polychaeta: Opheliidae) by established adults of
927 *Pseudopolydora paucibranchiata* (Okuda) (Polychaeta: Spionidae) on an intertidal sand flat. J Exp Mar Biol Ecol
928 87:67–82
- 929 Tamaki A (1987) Comparison of resistivity to transport by wave action in several polychaete species on an intertidal
930 sand flat. Mar Ecol Prog Ser 37:181–189
- 931 Tamaki A (1994) Extinction of the trochid gastropod, *Umbonium (Suchium) moniliferum* (Lamarck), and associated
932 species on an intertidal sandflat. Res Popul Ecol 36:225–236
- 933 Tamaki A, Harada K (2005) Alongshore configuration and size of local populations of the callianassid shrimp
934 *Nihonotrypaea harmandi* (Bouvier, 1901) (Decapoda: Thalassinidea) in the Ariake-Sound estuarine system, Kyushu,
935 Japan. Crustac Res 34:65–86
- 936 Tamaki A, Ingole B (1993) Distribution of juvenile and adult ghost shrimps, *Callianassa japonica* Ortmann
937 (Thalassinidea), on an intertidal sand flat: intraspecific facilitation as a possible pattern-generating factor. J Crustac
938 Biol 13:175–183
- 939 Tamaki A, Kikuchi T (1983) Spatial arrangement of macrobenthic assemblages on an intertidal sand flat, Tomioka Bay,
940 west Kyushu. Publ Amakusa Mar Biol Lab, Kyushu Univ 7:41–60
- 941 Tamaki A, Suzukawa K (1991) Co-occurrence of the cirrolanid isopod *Eurydice nipponica* Bruce & Jones and the ghost
942 shrimp *Callianassa japonica* Ortmann on an intertidal sand flat. Ecol Res 6:87–100
- 943 Tamaki A, Takeuchi S (2016) Persistence, extinction, and recolonization of an epibenthic gastropod population on an
944 intertidal sandflat: 35-y contingent history of a key species of the benthic community in metapopulation and
945 metacommunity contexts. J Shellfish Res 35:921–967
- 946 Tamaki A, Ueno H (1998) Burrow morphology of two callianassid shrimps, *Callianassa japonica* Ortmann, 1891 and
947 *Callianassa* sp. (= *C. japonica*: de Man, 1928) (Decapoda: Thalassinidea). Crustacean Res 27:28–39
- 948 Tamaki A, Harada K, Sogawa Y, Takeuchi S (2020a) Effect of stingray (*Hemirhynchus akajei*) foraging on a ghost shrimp
949 population (*Nihonotrypaea harmandi*) on an intertidal sandflat, western Kyushu, Japan. Mar Freshw Res
950 71:1128–1148

- 951 Tamaki A, Ingole B, Ikebe K, Muramatsu K, Taka M, Tanaka M (1997) Life history of the ghost shrimp, *Callinassa*
952 *japonica* Ortmann (Decapoda: Thalassinidea), on an intertidal sandflat in western Kyushu, Japan. J Exp Mar Biol
953 Ecol 210:223–250
- 954 Tamaki A, Itoh J, Hongo Y, Takeuchi S, Takikawa T (2018a) Normal delayed establishment of a semilunar brooding and
955 larval release cycle in the course of the reproductive season of the ghost shrimp population on a warm temperate
956 intertidal sandflat. J Shellfish Res 37:529–570
- 957 Tamaki A, Itoh J, Takeuchi S, Takikawa T (2020b) Semilunar postlarval settlement periodicity ensuing from semilunar
958 larval release cycle in the *Nihonotrypaea harmandi* (Crustacea, Decapoda, Axiidea, Callianassidae) population on an
959 intertidal sandflat in an open marine coastal embayment. Popul Ecol 62:161–195
- 960 Tamaki A, Kagesawa T, Takeuchi S, Ohashi H, Yang S, Sassa S (2018b) Facultative commensalism of a free-burrowing
961 urothoid amphipod with a deep burrow-dwelling callianassid shrimp in intertidal sand. Mar Biol 165:36
- 962 Tamaki A, Saitoh Y, Itoh J, Hongo Y, Sen-ju S, Takeuchi S, Ohashi S (2013) Morphological character changes through
963 decapodid-stage larva and juveniles in the ghost shrimp *Nihonotrypaea harmandi* from western Kyushu, Japan:
964 clues for inferring pre- and post-settlement states and processes. J Exp Mar Biol Ecol 443:90–113
- 965 Todd CD (1998) larval supply and recruitment of benthic invertebrates: do larvae always disperse as much as we
966 believe? Hydrobiologia 375/376:1–21
- 967 Tudhope AW, Scoffin TP (1984) The effect of *Callinassa* bioturbation on the preservation of carbonate grains in
968 Davies Reef lagoon, Great Barrier Reef, Australia. J Sediment Petrol 54:1091–1096
- 969 Volkenborn N, Reise K (2007) Effects of *Arenicola marina* on polychaete functional diversity revealed by large-scale
970 experimental lugworm exclusion. J Sea Res 57:78–88
- 971 Volkenborn, N, Robertson DM, Reise K (2009) Sediment destabilizing and stabilizing bio-engineers on tidal flats:
972 cascading effects of experimental exclusion. Helgol Mar Res 63:27–35
- 973 Wilson WH Jr (1979) Community structure and species diversity of the sedimentary reefs constructed by *Petaloproctus*
974 *socialis* (Polychaeta: Maldanidae). J Mar Res 37:623–641
- 975 Wilson WH Jr (1981) Sediment-mediated interactions in a densely populated infaunal assemblage: the effects of the

- 976 polychaete *Abarenicola pacifica*. J Mar Res 39:735–748
- 977 Wilson WH Jr (1989) Predation and the mediation of intraspecific competition in an infaunal community in the Bay of
978 Fundy. J Exp Mar Biol Ecol 132:221–245
- 979 Woodin SA (1981) Disturbance and community structure in a shallow water sand flat. Ecology 62:1052–1066
- 980 Woodin SA, Jackson JBC (1979) Interphyletic competition among marine benthos. Amer Zool 19:1029–1043
- 981 Wynberg RP, Branch GM (1994) Disturbance associated with bait-collection for sandprawns (*Callianassa kraussi*) and
982 mudprawns (*Upogebia africana*): long-term effects on the biota of intertidal sandflats. J Mar Res 52:523–558
- 983

984 **Figure captions**

985

986 **Fig. 1 a** Study region in mid-western Kyushu, Japan and location of intertidal sandflats (two boxes) along part of the
987 shoreline of Amakusa-Shimoshima (A.-S.) Island. Isobaths (10 m) by contouring (Surfer 8: Golden Software) for
988 point data from Hydrographic and Oceanographic Department, Japan Coast Guard. Tidal flats in black. **b** Tomioka
989 (intertidal) sandflat in gray and the area for monitoring of the benthic community during 1979–2019 in box. Rocky
990 or boulder areas in white. **c** Four shore-normal transects for the survey during 1979–1981, with Transect G used for
991 the subsequent census. The sandy part indicated in light gray. MLWS: mean low water level in spring tide periods.
992 The white 10-m wide zone along the upper shoreline: hard substrate during 1979–1991. The hatched 20-m wide
993 zone: area reclaimed during January 1991–March 1992, with the most landward sampling station on Transect G
994 shifted seaward by 20 m from 1992 onward. The four hatched plots near the MLWS line: breakwaters placed during
995 September 1993–December 1994. **d** Seven intertidal sandflats along the eastern shoreline of A.-S. Island (U1–U7 in
996 gray, with boulders or rocks in white). Two shore-normal transects on each of U1–U6 and three transects on U7 for
997 the census of the target benthic populations in 1998 in black lines, and transects on U2, U3, U5 and U6 and points on
998 U7 for the census in 2017–2018 in red lines and dots, respectively. Some boulder part in 1998 was covered with
999 sand in 2017–2018, now enabling sampling. See Tamaki and Takeuchi (2016) for details of the 1979–2014 situation

1000

1001 **Fig. 2 a, b** Close-up photographs of tube aggregations of the chaetopterid polychaete, *Mesochaetopterus minutus*, on
1002 Tomioka sandflat taken on March 1 and May 13, 2017, respectively. In panel b, scale range with value ticks: 36 cm.
1003 Burrow openings of the ghost shrimp, *Neotrypaea harmandi*, and a small feeding pit of the stingray, *Hemirytgon*
1004 *akajei*, seen in the lower and upper parts, respectively

1005

1006 **Fig. 3 a** Yearly change in mean (\pm SD) density of the ghost shrimp, *Neotrypaea harmandi*, over 16 (as a rule) stations
1007 on Transect G of Tomioka sandflat during 1979–2019, estimated from surface burrow-opening counts. For each year
1008 during 1979–2014, the putative October value (= actual value in the following March) given except for the

asterisked years with the summer value in each same year. The data for 1979–2014 adapted from Tamaki and
 Takeuchi (2016, fig. 11A–D). The value for 2014 identical to that for March 21, 2015, from which onward values on
 respective sampling occasions are indicated (Sp, spring; Su, summer). The combined data from March 1 and 30
 represented by the latter. The empirical threshold ghost shrimp density, 160 shrimp m^{-2} , above which gastropod
 recruitment is inhibited, indicated in horizontal broken line. **b** Yearly change in the abundance of the polychaete
 worm, *Mesochaetopterus minutus* (sum of the densities over all transect stations) during the study period. For each
 year during 1979–2014, the summer value given. From March 2015 onward, values on respective sampling
 occasions are indicated. **c** Yearly change in coefficient of permission by ghost shrimp [CP (shrimp→gastropod), with
 the value for March 21, 2015 identical to that for 2014] and coefficient of possible boost by worm for gastropod
 recruitment [CPB (worm→gastropod)]; see text for these coefficient definitions. **d** Yearly change in the abundances
 of the gastropod, *Umbonium moniliferum* [sum of densities over all transect stations for 0+ old cohort and for
 combined cohort (i.e., 0+ old cohort and 1+ and older (up to 3+) cohort; see Supplementary material 1)] during the
 study period. For each year during 1979–2014, the summer value given. From March 2015 onward, values on
 respective sampling occasions are indicated. Six links between year ($X - 1$) in panel c and year X in panel d
 illustrated in arrowed dotted lines, with black for CP [plus, promotion; minus, inhibition with (almost) zero CP] and
 red for CPB (plus, promotion). Note that (1) each year from 1979 to 2014 in panel d is aligned with its previous year
 in panels a–c so that a possible influence from ghost shrimp or worm on gastropod recruitment within each same
 year can easily be traced [i.e., the abundance of gastropod’s 0+ old cohort in the summer of year X reflects that of
 newly-recruited gastropods in October of year ($X - 1$) and thus mean (\pm SD) of ghost shrimp in putative October and
 the abundance of worm in summer are plotted on the ($X - 1$)-year tick], (2) for the period from March 2015 to
 August 2019, each real sampling occasion is aligned across all panels, and (3) between 2014 and 2015Sp, the year-
 tick positions are adjusted between panels a–c and panel d

Fig. 4 a, b, c–k Spatial variations in the densities of ghost shrimp (*Neotrypaea harmandi*; estimated from surface
 burrow-opening counts), polychaete worm (*Mesochaetopterus minutus*), and gastropod (*Umbonium moniliferum*; 0+

old and 1+ and older cohorts, based on Supplementary material 4) at 16 (as a rule) stations along Transect G on Tomioka sandflat in 2010 and during 2015–2019, respectively. The empirical threshold ghost shrimp density, 160 shrimp m^{-2} above which gastropod recruitment is inhibited, indicated in shade in panel a. The data for 2010 adapted from Tamaki et al. (2018b, fig. 5c) and Tamaki and Takeuchi (2016, figs. 10 and 13). In panels a and b, except for the March 2017-data (panel a) and for the May 2016- and March 2017-data (panel b), the summer data indicated for each year. MLWS: mean low water level in spring tide periods

Fig. 5 a Thickness of sand column (mean of five data) at each of five stations along Transect G on Tomioka sandflat on August 3, 2016. **b** Densities of ghost shrimp (*Neotrypaea harmandi*) at the five stations on August 3, 2016 for (1) first 0-y cohort [4.1 to 12.1-mm total length (TL)], combined cohort from 1- and 2-y ones (21.1 to 34.1-mm TL), and combined cohort from all ones in ten sediment cores (total area, 1,000 cm^2 ; values from 11 samples at Stn 30 converted to it) and (2) whole population, estimated from surface burrow-opening counts on August 1. **c** Densities of ghost shrimp at the five stations on May 27, 2017 for second 1-y cohort (derived from recruits in autumn 2016), first 1-y cohort (recruits in summer 2016, derived from first 0-y cohort in panel b plus those recruited after that by the end of August), 2-y cohort (recruits in 2015), and combined cohort from all ones. The TL-frequency distributions for these cohorts given in Supplementary material 3. MLWS: mean low water level in spring tide periods

Fig. 6 a,b Areal inverse-distance-weighted interpolation for the densities of the polychaete worm (*Mesochaetopterus minutus*) and the ghost shrimp (*Neotrypaea harmandi*) around the mid-tidal zone of Tomioka sandflat on August 1 and 2, 2016, respectively. Cross marks: sampling stations including those from Stn 90 to Stn 250 on Transect G. See the Materials and methods in text for details of field sampling and laboratory interpolation procedures

Fig. 7 a–c Spatial variations in median particle diameter ($Md\phi$), sorting coefficient (inclusive graphic standard deviation, σ_1), and silt-clay content (<0.063 mm in diameter) of the surface 1-cm sediment at 16 (as a rule) stations along Transect G on Tomioka sandflat in 2010 and during 2015–2018, respectively (3-cm sediment in 2015). Data

1059 for 2010 adapted from Tamaki et al. (2018b, fig. 6) in broken line connecting plots. Except for the March 2017-data
1060 in solid line connecting plots, the summer data indicated for each year. MLWS: mean low water level in spring tide
1061 periods. **d** Ground heights of the sandflat surface relative to mean sea level in Tokyo Bay on the transect in each
1062 summer of 2015, 2016, and 2017. **e** Spatial variations in vane shear strengths at 1-cm and 4-cm depths of the surface
1063 sediment on the transect in each summer of 2015 and 2016 and in spring 2017. **f** Vane shear strengths at 1-cm depth
1064 inside and outside polychaete worm (*Mesochaetopterus minutus*) aggregations around the blue circle point in Fig.
1065 9b, corresponding to varying groundwater tables

1066
1067 **Fig. 8 a** Plots for the mean value, over the stations on Transect G of Tomioka sandflat, of the absolute difference in σ_1
1068 between 1-cm and 3-cm surface sediments at each station versus the mean value of such differences in $Md\phi$ in each
1069 summer of 2010, 2016, 2017, and 2018 and spring of 2017. Data for 2010 based on Tamaki et al. (2018b, fig. 6 for
1070 1-cm depth) and A. Tamaki (unpubl data for 3-cm depth). **b** Estimated daily reduction rates in ghost shrimp
1071 (*Neotrypaea harmandi*) density at Stns 30, 90, 150, 210, and 270 on Transect G from March to July (August) in
1072 2010, 2015, and 2017 and from May to August in 2016. Data for 2010 based on Tamaki et al. (2018b, fig. 13 for
1073 March 30) and A. Tamaki (unpubl data for August 11). Used for each month of 2010, 2015, and 2017 in the
1074 calculation is the mean value of the mean shrimp densities (estimated from surface burrow openings) at the three
1075 successive stations centered at each of the above five stations (specifically for Stn 270, Stns 250 and 270 adopted).
1076 For the density of combined 1+- and 2+-y cohort at each station in August 2016, the proportion of that cohort in the
1077 sediment-core samples (Fig. 5b) is used to estimate that cohort's density based on the total burrow-opening counts

1078
1079 **Fig. 9 a,b** Ground height isobaths (relative to mean sea level in Tokyo Bay) interpolated with Surfer 12 (Golden
1080 Software) for a rectangular area of Tomioka sandflat containing Transect G (stations in blue) in each summer of
1081 2015 and 2016, respectively. **c** Isobaths with a higher resolution for part of the area in panel b (2016-strip: left panel)
1082 and in its adjacent 2017-strip (right), respectively, both containing the segment from Stn 150 to Stn 170 on Transect
1083 G. In the 2016-strip, three dimensions in ellipsoid (long axis \times short axis \times maximum height) for the three distinct

1084 elevations in the seaward half: from left to right, 8.4 m × 6.4 m × 8 cm, 9.0 m × 5.5 m × 3 cm, and 7.0 m × 4.6 m × 7
1085 cm. The leftmost distinct depression (ellipsoid) in the landward half: 7.6 m × 5.8 m × 5 cm (maximum depth). **d**
1086 Aerial photograph from 32-m height, centered at the blue circle point in panel b, in August 2016. **e** Ground-height
1087 isobaths around one worm aggregation in the red square plot in panel b in August 2016

1088
1089 **Fig. 10 a** Drift card release points (blank stars) in October 2008 and their presumed corresponding sandflats with
1090 populations of *Umbonium moniliferum* (solid circles tied to stars) in Amakusa-Shimoshima Island. The Un ($n = 1$ to
1091 7) sandflats the same as those given in Fig. 1d. Red line and red triangle point in the inset: upper shoreline part of
1092 Tomioka sandflat used for card retrieval and point of wind velocity recording by Kumamoto Prefecture Government,
1093 respectively. **b** Daily cumulative numbers of retrieved cards derived from the star points in panel a after the release
1094 (Release-1; upper row), tidal height changes with time at Nagasaki Harbor 30 km north of Tomioka Bay recorded by
1095 Japan Meteorological Agency (middle row), and wind velocity changes with time recorded at the red triangle point
1096 in panel a, inset (lower row). The syzygy date prior to Release-1: September 29. **c** Data sets for the two card-releases
1097 in October 2009 similar to those for 2008 in panel a,b (Release-2 group in black; Release-3 group in red, with solid
1098 circles derived from the ‘offshore’ release point and open circles from the ‘nearby sandflat’ release point in Tomioka
1099 Bay, respectively; lines for R3-1-2 adapted from Mandal et al. 2010, fig. 11). The quadrature date prior to Release-2:
1100 October 3. Two breaks with no card retrieval in the lines with no dots. Parentheses: cards picked up by a person of
1101 the local town on one date and handed to us (no retrieval made ourselves on that date)

1102

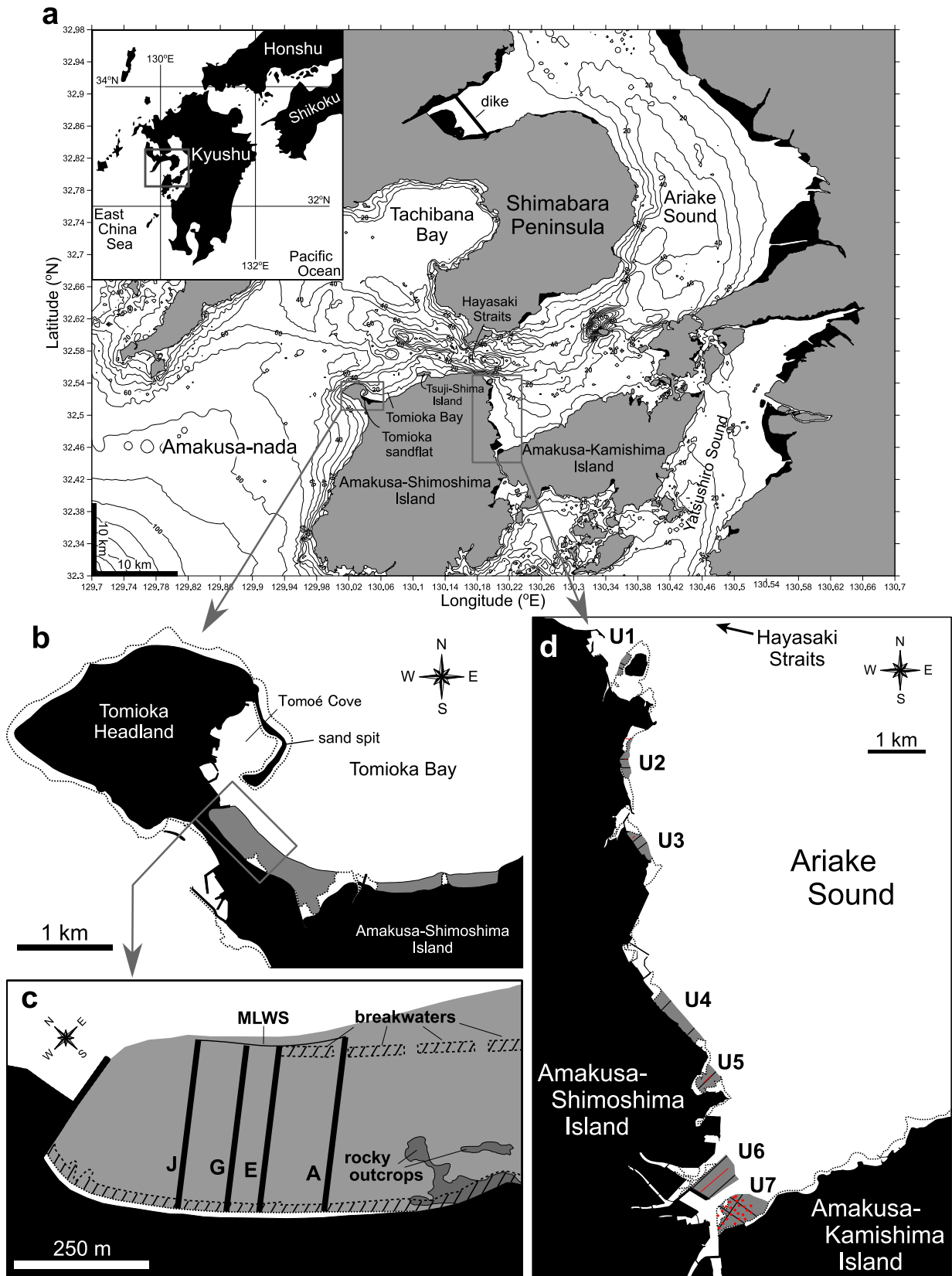


Fig. 1 (Tamaki et al., revised)



Fig. 2 (Tamaki et al., revised)

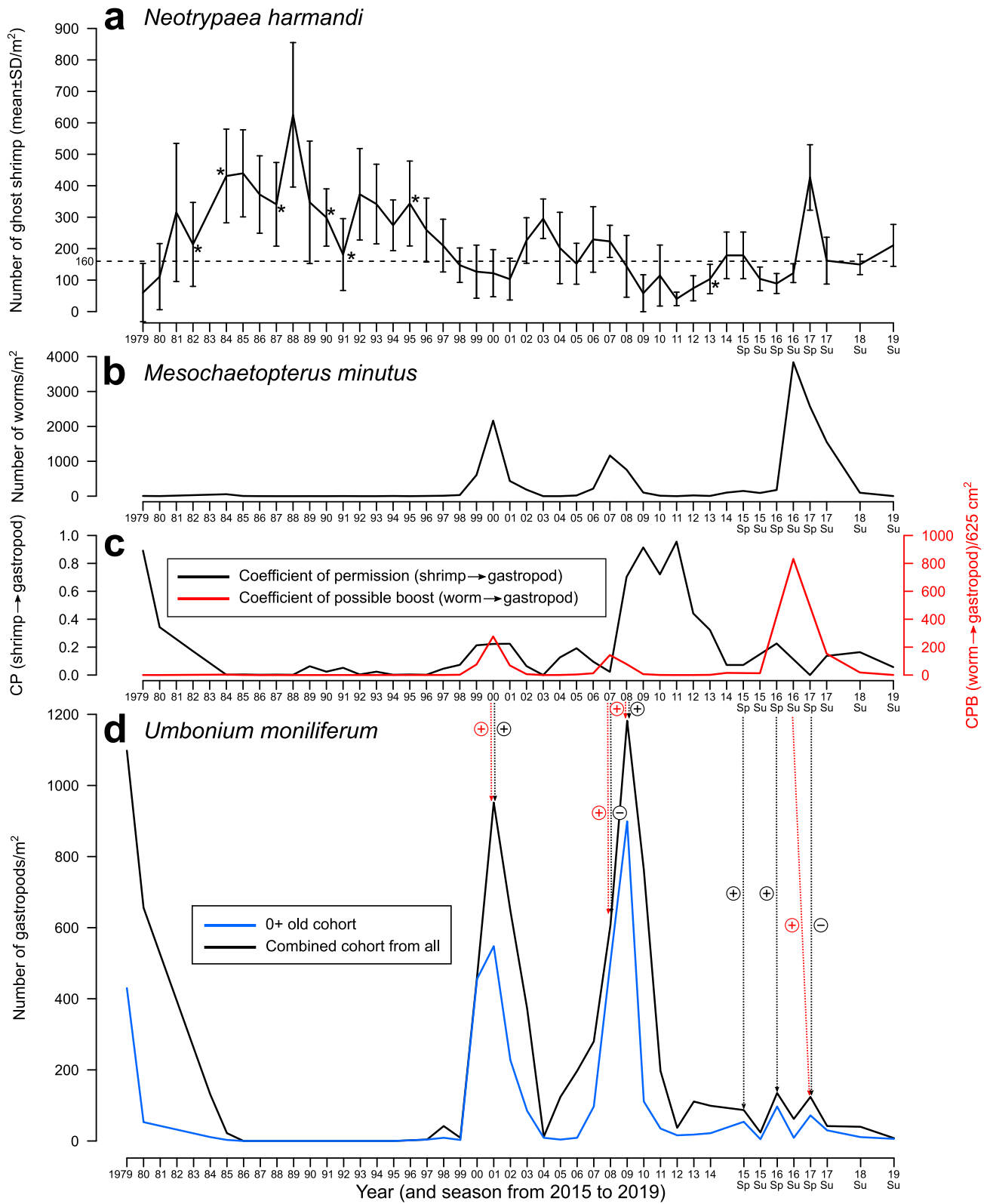


Fig. 3 (Tamaki et al., revised)

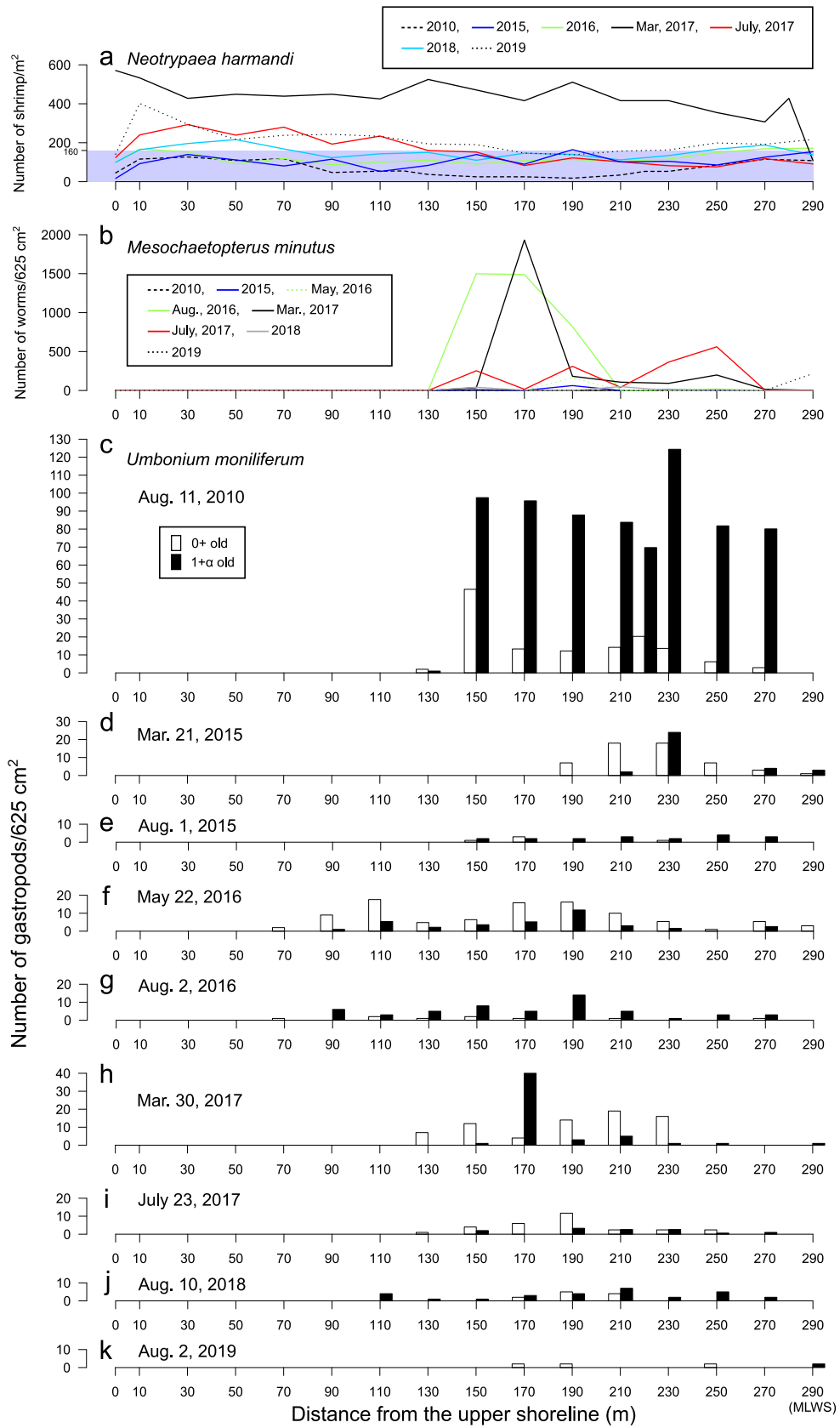


Fig. 4 (Tamaki et al., revised)

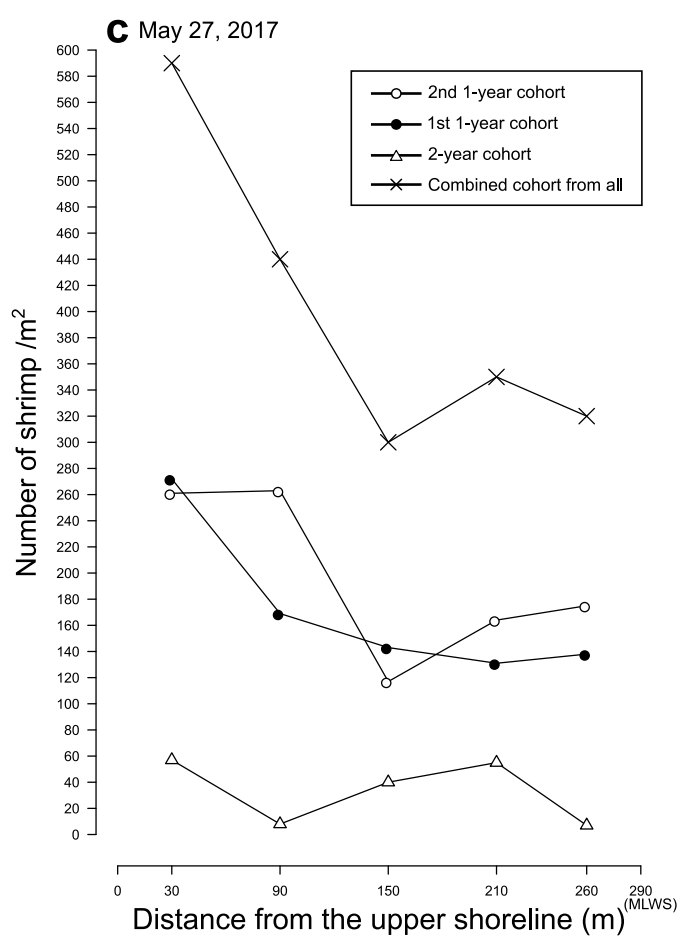
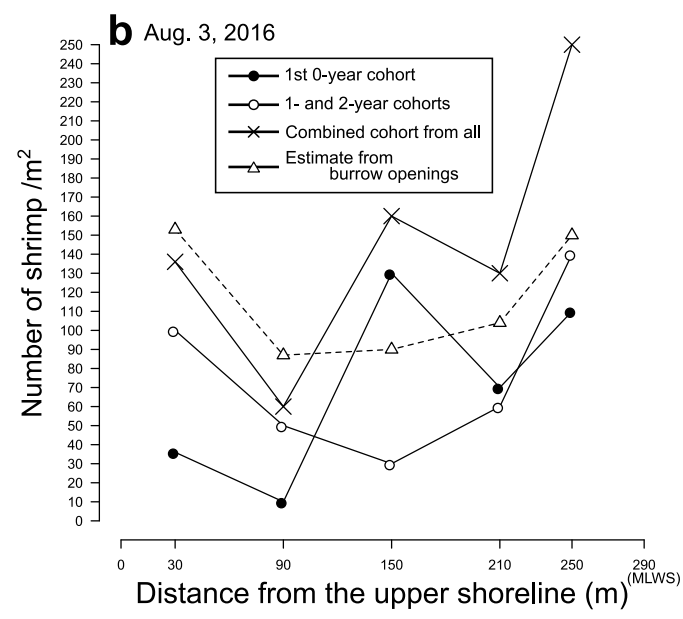
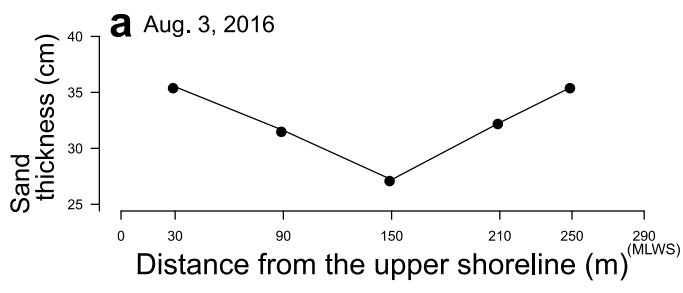


Fig. 5 (Tamaki et al., revised)

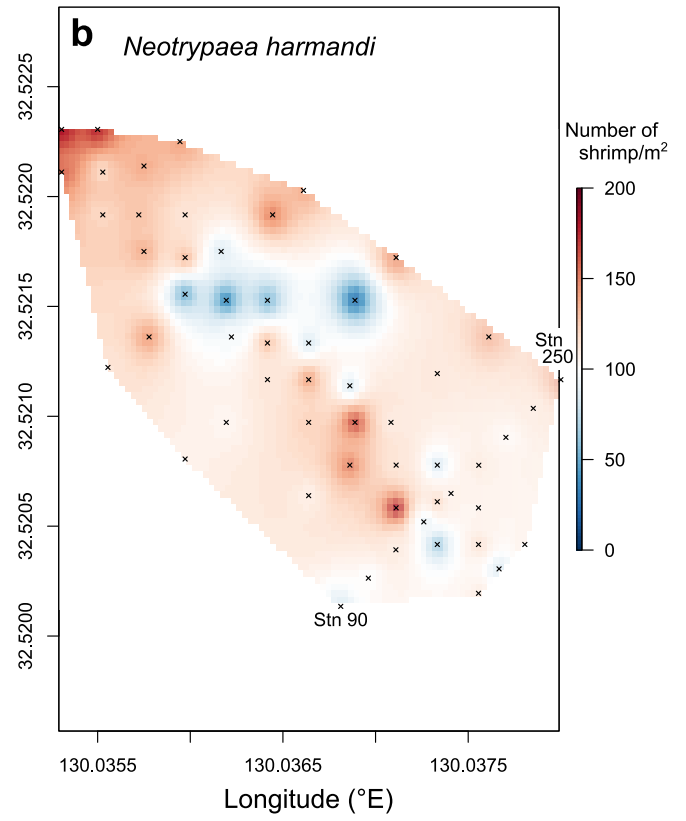
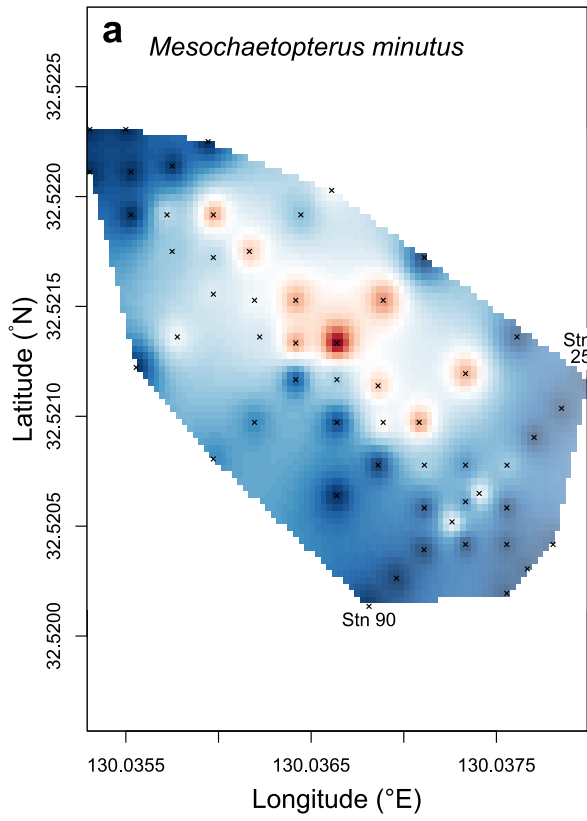


Fig. 6 (Tamaki et al., revised)

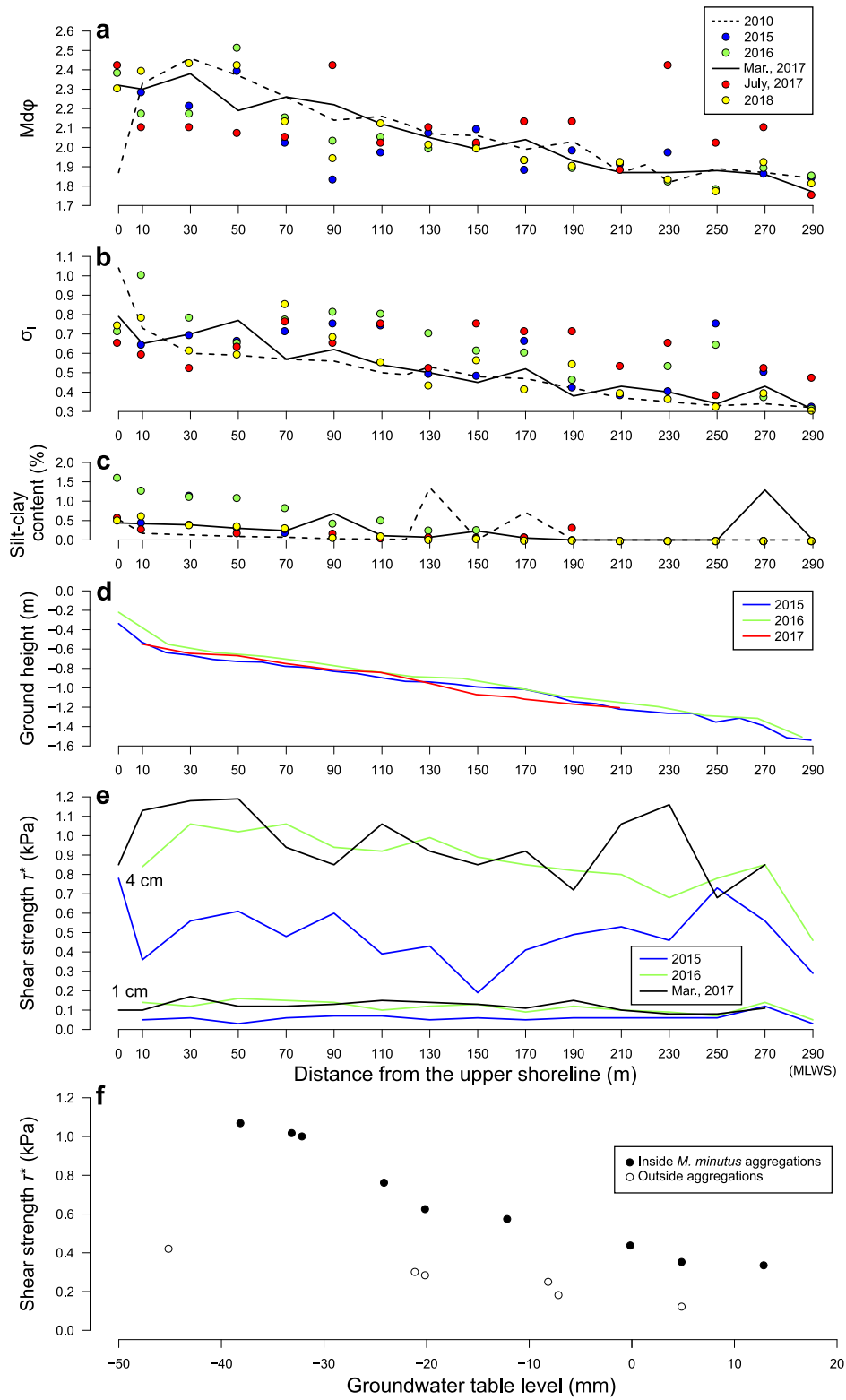


Fig. 7 (Tamaki et al., revised)

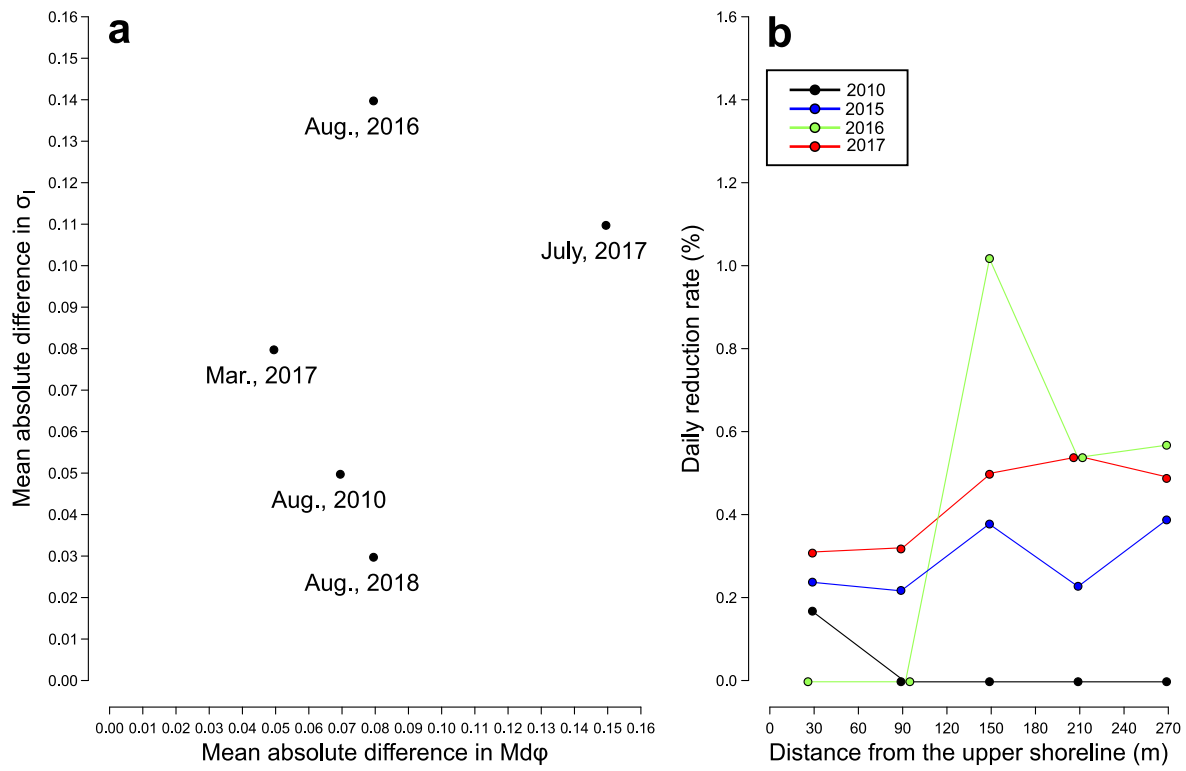


Fig. 8 (Tamaki et al., revised)

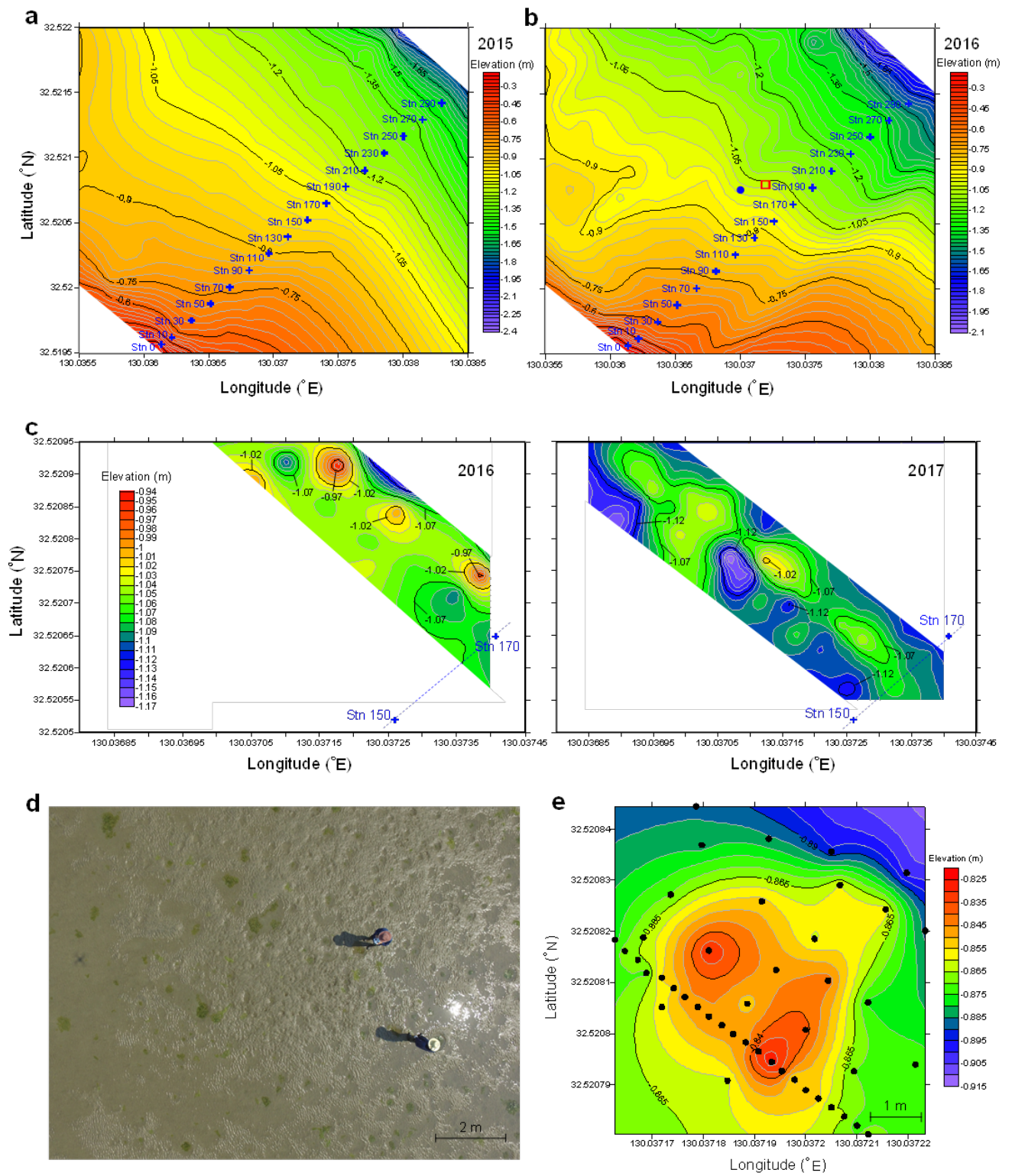


Fig. 9 (Tamaki et al., revised)

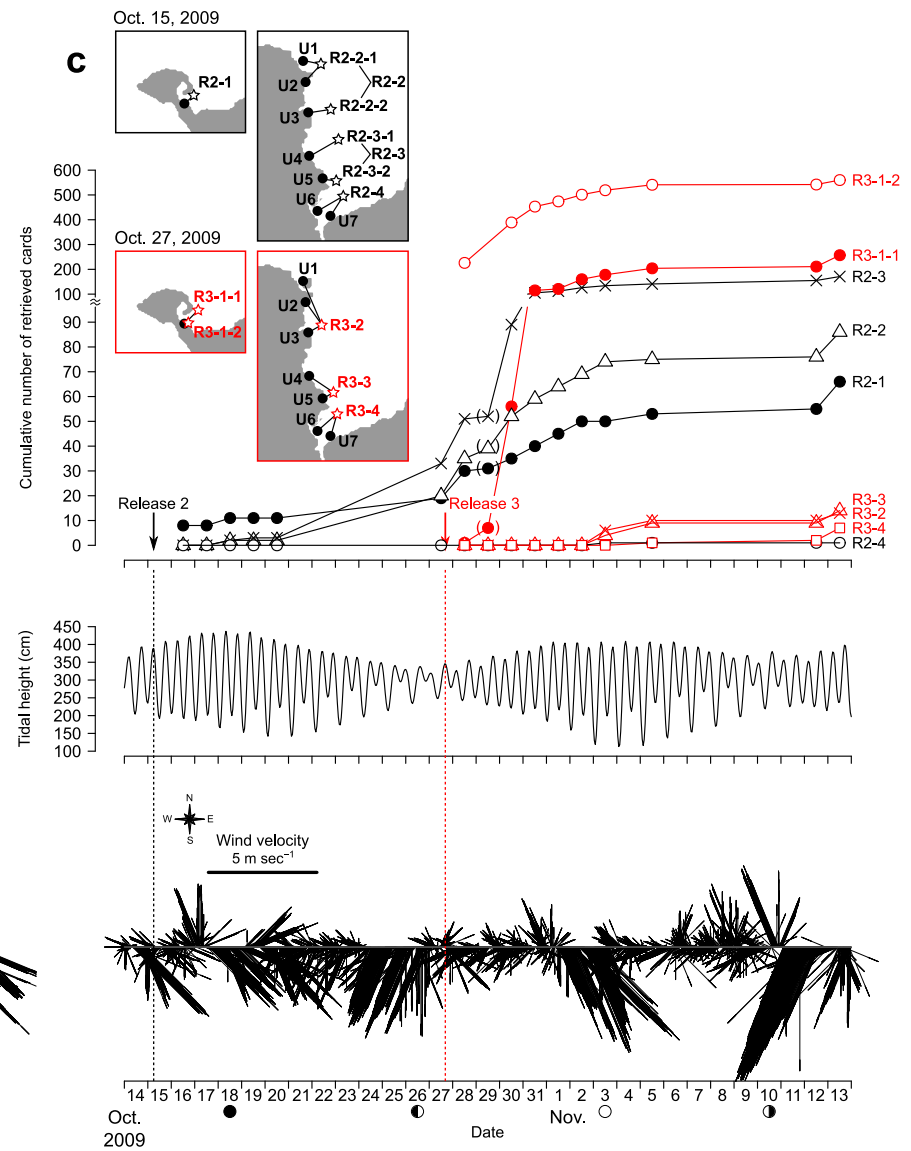
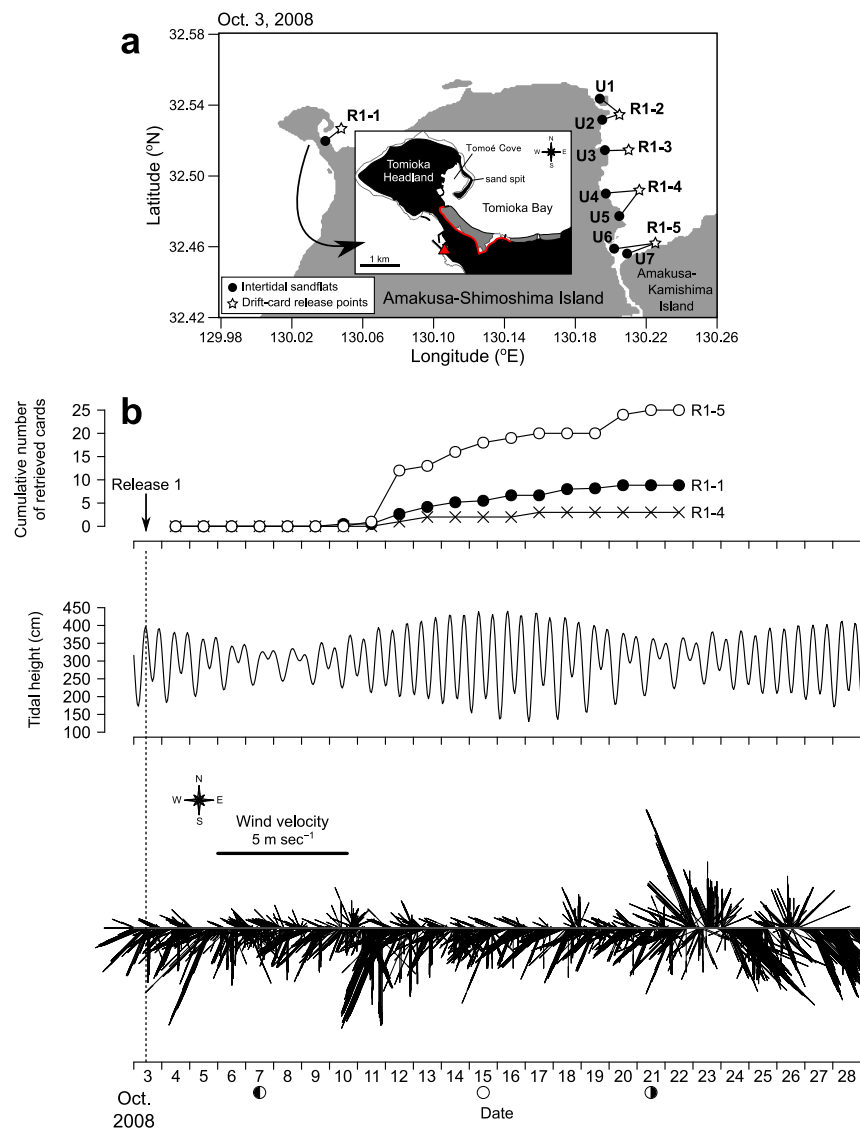


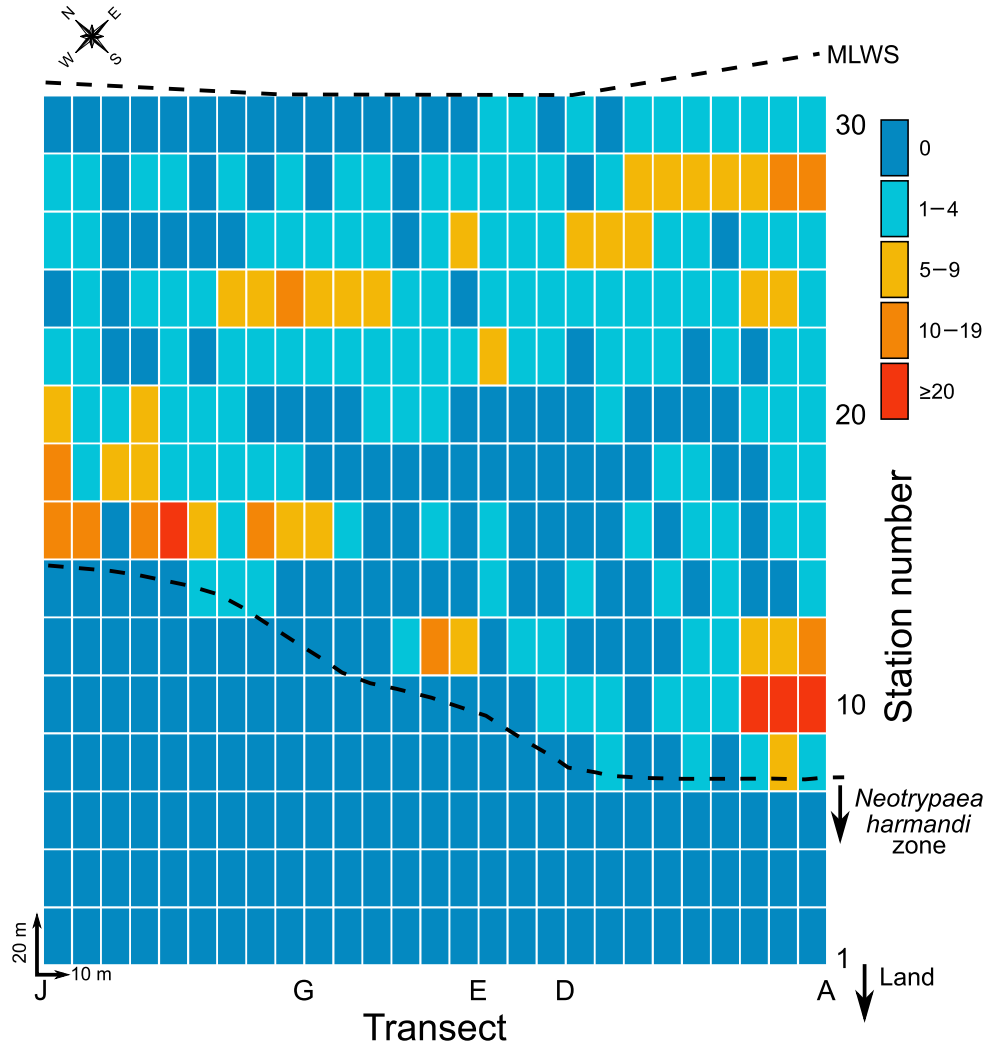
Fig. 10 (Tamaki et al., revised)

Supplementary material 1: Biology, life history, and population dynamics of the gastropod *Umbonium moniliferum*

Sources of information: Tamaki (1994), Harada et al. (2005), Mandal et al. (2010), and Tamaki and Takeuchi (2016). On Tomioka sandflat, the average individual density in each summer of 1979, 2001, and 2009 was 1900–2500 gastropods m^{-2} . Mass spawning of dioecious gametes occurs discretely, centered at each of the three serial neap tide periods mainly in October. An individual female can successively produce those three batches of eggs. It takes a minimum of 3 d for lecithotrophic planktonic larvae to settle on the sandflat and metamorphose into the juvenile at 0.2-mm shell width. A batch of newly-fertilized embryos in the laboratory decreased according to the equation, $y = 31.647 \times 0.664^x$, with y the proportion of the initial larval number on Day x ($2 < x \leq 9$). On the sandflat, a batch of synchronously fertilized embryos settle substantially by Day 9. The three benthic juvenile cohorts merge into a single cohort by April. In the subsequent autumn, members of that cohort reproduce at the smallest shell width of 5 mm (0+ old adult cohort). The 0+ old cohort is mostly well separated from the 1+ and older cohorts (with 3-y life span) in their shell width-frequency distribution. In 1979, when *N. harmandi* was non-limiting to *U. moniliferum* on Tomioka sandflat due to their separate distributions, the gastropod population was estimated to be a demographic sink in the regional metapopulation, requiring larval supply from other local populations. Ten intertidal sandflat populations in Ariake Sound were regarded as candidates sending larvae to the Tomioka population during its recovery phases in the 2000s. Six local populations on the eastern shoreline of A.-S. Island were most likely candidates (on U2 to U7 sandflats in Fig. 1d in text); in 1998, (a) when mean population density on Tomioka sandflat was 74 gastropods m^{-2} , those values on U1 to U7 sandflats were 22, 928, 1025, 607, 771, 1204, and 1075, respectively; (b) estimated population sizes ($\times 10^5$) on Tomioka sandflat and these U_n ($n = \text{identity number, 1 to 7}$) sandflats were 72, 7, 770, 1035, 1325, 779, 3372, and 3955; and (c) mean densities of surface burrow openings of *N. harmandi* on Tomioka sandflat and these U_n sandflats were 537, 406, 46, 85, 73, 55, 59, and 57 counts m^{-2} (Tamaki and Harada 2005). Note that in addition to *N. harmandi*, only on U6 and U7 sandflats occurred its congener, *N. japonica* with a single surface burrow opening (Tamaki and Ueno 1998) and their inclusive burrow-opening densities given above.

References:

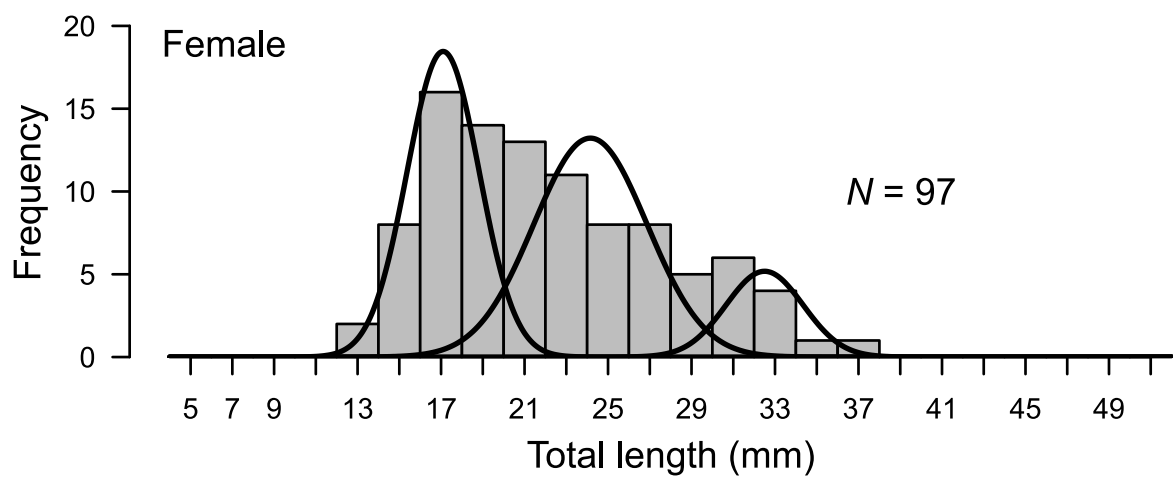
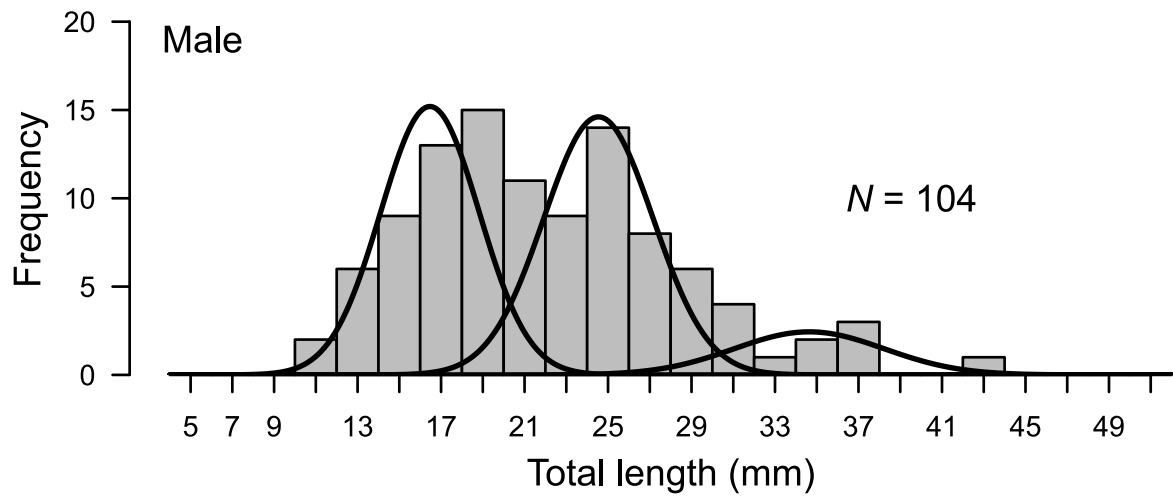
- Harada K, Ohashi S, Fujii A, Tamaki A (2005) Embryonic and larval development of the trochid gastropod *Umbonium moniliferum* reared in the laboratory. *Venus (Jpn J Malacol)* 63:135–143
- Mandal S, Tamaki A, Ohashi S, Takeuchi S, Agata Y, Takahara Y, Harada K, Yamada F (2010) How newly recruited cohorts are formed in the trochid gastropod population (*Umbonium moniliferum*) on an intertidal sandflat in western Kyushu, Japan. *J Exp Mar Biol Ecol* 389:18–37
- Tamaki A (1994) Extinction of the trochid gastropod, *Umbonium (Suchium) moniliferum* (Lamarck), and associated species on an intertidal sandflat. *Res Popul Ecol* 36:225–236
- Tamaki A, Harada K (2005) Alongshore configuration and size of local populations of the callianassid shrimp *Nihonotrypaea harmandi* (Bouvier, 1901) (Decapoda: Thalassinidea) in the Ariake-Sound estuarine system, Kyushu, Japan. *Crustac Res* 34:65–86
- Tamaki A, Takeuchi S (2016) Persistence, extinction, and recolonization of an epibenthic gastropod population on an intertidal sandflat: 35-y contingent history of a key species of the benthic community in metapopulation and metacommunity contexts. *J Shellfish Res* 35:921–967
- Tamaki A, Ueno H (1998) Burrow morphology of two callianassid shrimps, *Callianassa japonica* Ortmann, 1891 and *Callianassa* sp. (= *C. japonica*: de Man, 1928) (Decapoda: Thalassinidea). *Crustacean Res* 27:28–39



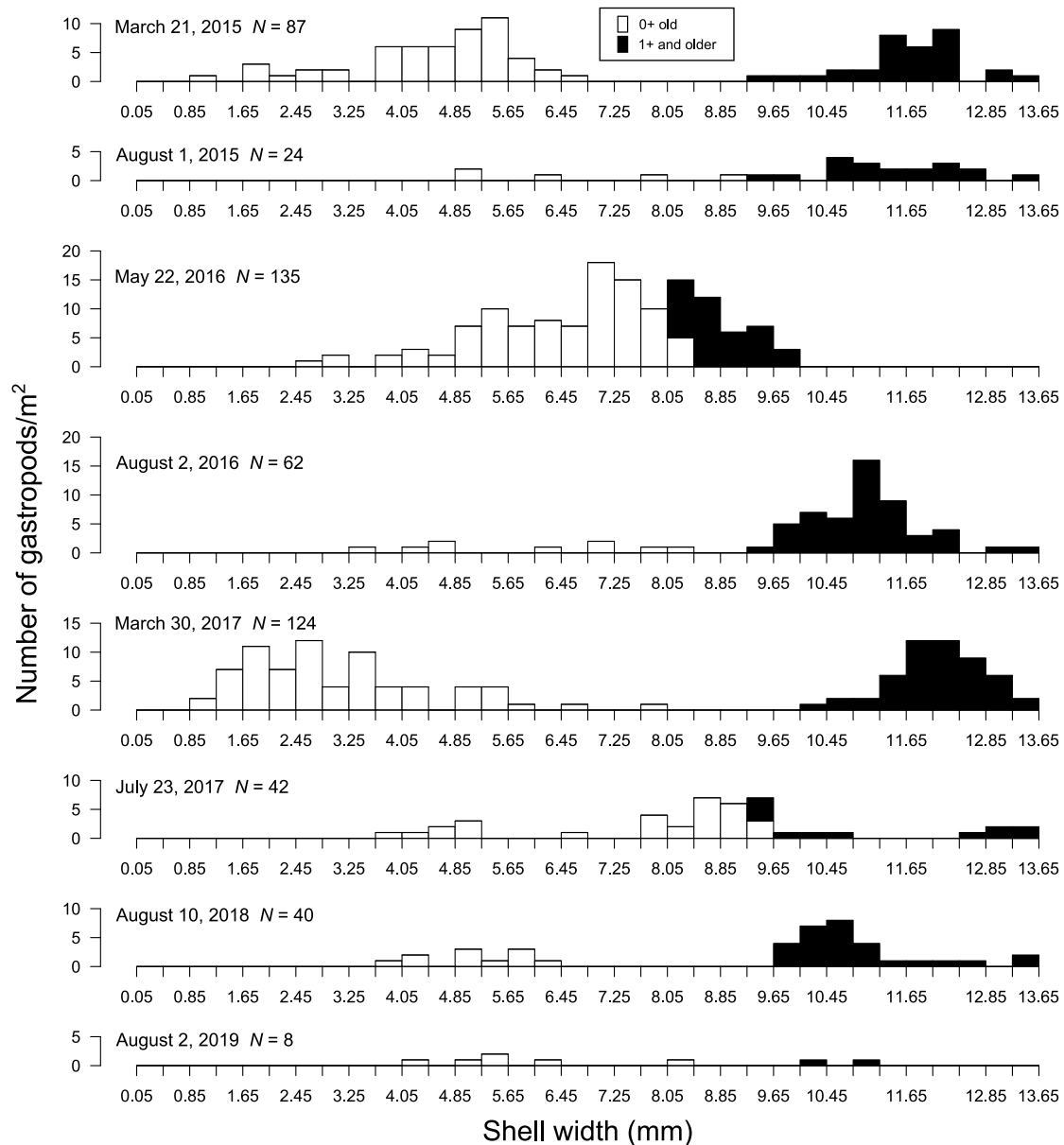
Supplementary material 2 Distribution of mounds of the chaetopterid polychaete worm, *Mesochaetopterus minutus*, in July 1979 over the area between Transects A and J on Tomioka sandflat [Fig. 1c in text; adapted from Tamaki and Kikuchi (1983, fig. 4)]. MLWS: mean low water level in spring tide periods. The distance between two adjacent benthos-collection points on each transect is 10 m. The area was divided into rectangular cells for worm density survey, each with 20-m (shore-normal) × 10-m (alongshore) sides. Worm mound numbers per cell were assigned to one of the five classes. Ghost shrimp (*Neotrypaea harmandi*) distribution was limited to landward of the broken line, with mean (\pm SD) density estimated from burrow opening counts at the points containing any one opening on the four transects being 164.2 ± 93.7 shrimp m^{-2} ($n = 38$). No worm mounds were in the shrimp zone, whereas 17 cells with mounds fringed the seaward edge of that zone. In all cells seaward of the shrimp zone ($n = 278$), the proportions of the five classes of worm density, from low to high, were 38.5, 46.4, 10.1, 3.6, and 1.4%. With each class median density (20 for the class ≥ 20), the grand mean mound density was estimated to be 2.67 mounds per 200 m^2 . During 1979 to 2014, worm density per benthos-collection point was monitored along Transect G (Tamaki and Takeuchi 2016). Until 1998 there were no mounds, with a high of 56 worms m^{-2} . Densities spiked to 16400 and 14800 worms m^{-2} on the mid-transect in 2000 and 2007, respectively.

References:

- Tamaki A, Kikuchi T (1983) Spatial arrangement of macrobenthic assemblages on an intertidal sand flat, Tomioka Bay, west Kyushu. Publ Amakusa Mar Biol Lab, Kyushu Univ 7:41–60
- Tamaki A, Takeuchi S (2016) Persistence, extinction, and recolonization of an epibenthic gastropod population on an intertidal sandflat: 35-y contingent history of a key species of the benthic community in metapopulation and metacommunity contexts. J Shellfish Res 35:921–967



Supplementary material 3 Total length-frequency distributions of male and female of the ghost shrimp population (*Neotrypaea harmandi*) per 5000-cm² area of Tomioka sandflat on May 27, 2017, with ten 100-cm² sediment-core samples from each of Stns 30, 90, 150, 210, and 260 on Transect G (Fig. 1c in text) combined. The fitted normal-distribution curves stand for 2-y cohort, first 1-y cohort, and second 1-y cohort from right to left



Supplementary material 4 Temporal change in shell width-frequency distribution of the gastropod population (*Umbonium moniliferum*) from the combined, 16 (as a rule) stations along Transect G on Tomioka sandflat (Fig. 1c in text) during 2015–2019. The 0+ old and 1+ and older cohorts were separated, based on Tamaki and Takeuchi (2016, fig. 10). For the distributions in May 2016 and July 2017, with some overlap in shell width between the two cohorts, the gastropod number of 0+ old cohort in its possible maximum shell-width class was estimated by linear interpolation between the total number in its left adjacent class and zero in its right adjacent class.

Reference:

Tamaki A, Takeuchi S (2016) Persistence, extinction, and recolonization of an epibenthic gastropod population on an intertidal sandflat: 35-y contingent history of a key species of the benthic community in metapopulation and metacommunity contexts. *J Shellfish Res* 35:921–967

Supplementary material 5

Estimation for the proportional contribution of the cards (as virtual larvae) reaching Tomioka sandflat ‘alive’ from Tomioka itself and those from each combined population group of the Un sandflats in A.-S. Island to all cumulative ‘survivor cards’ during the period from Day 3 (shortest gastropod PLD) to Day 9 (substantial surviving duration)

Based on a data set about (a) number of daily retrieved cards derived from each release point (number of released cards per point = 800) corresponding to the respective, combined sandflat populations at Release-3 (Fig. 10c in text), (b) daily larval survival rates in the laboratory rearing [$y = 31.647 \times 0.664^x$, with y being the proportion of the initial larval number on Day x ($2 < x \leq 9$) (Supplementary material 1)], and (c) estimates for the local population sizes of Tomioka and Un sandflats for the year of 1998 [ratios of Tomioka: (U1 + U2 + U3): (U4 + U5): (U6 + U7) = 1: 25.3: 29.3: 102.2 (Supplementary material 1)], each proportional contribution was calculated as $\Sigma [(a) \div 800 \times (b)]$ (for Days 3–7 and 9; no data on Day 8) \times [proportional population size of Tomioka sandflat or each Un -sandflat group in the sum of the population sizes in (c)]. Computation was made separately for the two card-release points in Tomioka Bay. From R3-1-2 point (closer to the sandflat), 226 cards were retrieved on Day 1, which should have returned offshore if they were the real, still incompetent (for settlement) larvae; the small number of cards on Day 2 is negligible. A correction was made for this on the assumption that (1) stranding of those ‘live cards’ on Tomioka sandflat was postponed to the period from Day 3 to Day 9 and (2) those cards were retained within Tomioka Bay during that period albeit full retention would not be achieved (Tamaki et al. 2018). To illustrate, on Day 3, 163 cards were actually stranded. The corrected number for that date was estimated to be 227 [= $163 + 226 \times 163 \div (800 - 226)$]. A similar correction was made for the subsequent dates: 89 on Day 4 [= $64 + 226 \times 64 \div (800 - 226)$], 29 (Day 5), 38 (Day 6), 25 (Day 7), and 31 (Day 9). Such corrections are necessary only for the card releases from Tomioka Bay because of the later arrival of the cards from off Un s. The proportion of the total ‘survivor cards’ from each of the two release points in Tomioka Bay (R3-1-2 and R3-1-1) to all ‘survivor cards’ including the ones from the three release points off the corresponding three Un groups was estimated to be 79.1% and 56.3%, respectively. When the above-mentioned assumption (2) was not fully satisfied, these proportion values become lower to some extent. The proportional contribution from each Un group was estimated in a similar way.

Reference:

Tamaki A, Itoh J, Hongo Y, Takeuchi S, Takikawa T (2018) Normal delayed establishment of a semilunar brooding and larval release cycle in the course of the reproductive season of the ghost shrimp population on a warm temperate intertidal sandflat. *J Shellfish Res* 37:529–570